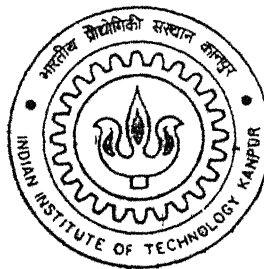


Mixed Convection Cooling for PCB Type Configurations

By

Akhilesh Kumar Singh



TH
ME/2002/M
Si 64 m

DEPARTMENT OF MECHANICAL ENGINEERING

Indian Institute of Technology Kanpur

JANUARY, 2002

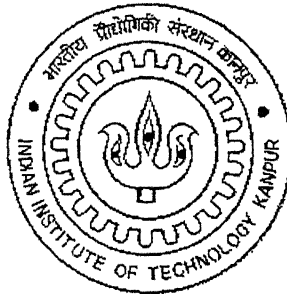
Mixed Convection Cooling for PCB Type Configurations

*A Thesis Submitted
In Partial Fulfillment of the Requirements
For the Degree of*

Master of Technology

by

Akhilesh Kumar Singh



to the

**DEPARTMENT OF MECHANICAL ENGINEERING
INDIAN INSTITUTE OF TECHNOLOGY KANPUR**

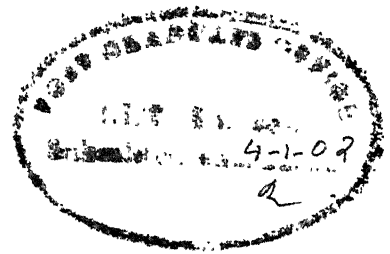
JANUARY 2002

26 APR 2002

117E
दुष्पोत्तम काशीनाथ केलकर पुस्तकालय
भारतीय प्रौद्योगिकी संस्थान कानपुर
अवधि क्र० A 139578



A139578



Certificate

It is certified that the work contained in the thesis entitled '*Mixed convection cooling for PCB type configurations*' by **Mr. Akhilesh Kumar Singh (Y010505)**, has been carried out under my supervision and this work has not been submitted elsewhere for a degree.

Keshav Kant

Jan 01, 2002

(Dr. Keshav Kant)

Professor,

Department of Mechanical Engineering,

Indian Institute of Technology,

Kanpur 208 016

January, 2002

Acknowledgements

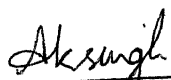
I would like to express my deep sense of gratitude to Dr. Keshav Kant for his inspiring and valuable guidance during the period of this work. I will remain indebted for the care and the affection he has showered on me.

I would like to dedicate this work to my parents, brothers and sisters for their enduring love, support and inspiration.

I am sincerely thankful to Mr. Vipin for his support and suggestions. I owe a lot to him, without him this project would not have been possible. I shall be failing in my duties if I do not express my gratefulness and thanks to Mr. Sushil Mishra, Mr. D.S. Murthy, Mr. Ashok Pise, Mr. H. K. Paliwal and my friends Nikhil, Ramesh, Satish, Ramanand, Narm, Lalit, Girdhari, Vikas, Subodh, Pankaj for their invaluable help and providing me with a vivacious atmosphere during my stay at this institute.

Last but not the least I would like to express my gratefulness to all those who directly or indirectly helped me through successful completion of my work.

I.I.T. Kanpur


(Akhilesh Kumar Singh)

Date: 04/04/2002

Abstract

With progressive miniaturization in integration technology in the electronic industry, intense efforts are being made in the design and development of printed circuit boards to enhance the capability of dissipating the enormous amount of heat flux generated by components mounted over them.

The present experimental work has emphatically targeted to simulate printed circuit board type heated plate configurations. Such configurations are often used in numerous electronic devices like main frame computers, personal computers and more sophisticated modern data processing devices. This study has been done with uniform surface temperature condition for the heated plate.

The experimental data which has been acquired in considerable volume helps in visualizing the trends in various thermal parameters like surface heat flux, total heat dissipated during the cooling, Nusselt number, etc. with relative variation in physical parameters like plate spacing, channel height etc. These data can be used as a preliminary basis for estimating the cooling performance of a printed circuit board and also for designing such boards with given number of heat generating chips and other elements over them. The experimental results have been compared with the theoretical and numerical results for the similar configurations and a few empirical relations for the design purposes are suggested.

Contents

Certificate	: i
Acknowledgements	: ii
Abstract	: iii
Contents	: iv
Nomenclature	: v
List of Figures	: vi
Chapter-1 General background	: 1
Chapter-2 Literature survey	: 10
Chapter-3 Problem description and experimental set-up	: 30
Chapter-4 Results and discussion	: 45
References	: 65

Nomenclature

A_T	Activation energy
Bo_y	Boussinesq number measured along y
E_a	Characteristic activation energy
Gr	Grashoff number
K_B	Boltzman constant
Nu	Nusselt number
Pe_y	Peclet number measured along y
Re	Reynolds number
Ra	Rayleigh number
Q	Heat Flux
T	Temperature, K
X	Plate Spacing, mm
X_{op}	Optimum plate spacing, mm
Q_{op}	Optimum heat flux, Wcm^{-2}
g	Gravitational acceleration, ms^{-2}

List of Figures

- Figure 1.1 a** Electronic enclosure
- Figure 1.1 b** Chips mounted on the board
- Figure 1.1 c** Heat generating chip
- Figure 1.2 a** Heat transfer in an electronic component
- Figure 1.2 b** Path of Heat transfer
- Figure 1.3** Flow chart for cooling of a PCB
- Figure 2.1** Schematic of the test rig used by Tiwari and Jaluria
- Figure 2.2** Ligranie's setup for mixed convection in straight and curved channels
- Figure 2.3** Schematic of the test rig used by Maughan
- Figure 2.4** Schematic of previous setup used by Maughan
- Figure 2.5** Schematic of setup used by Ramchandran
- Figure 3.1** Experimental setup
- Figure 3.2** Experimental test rig
- Figure 3.3** Air intake unit
- Figure 3.4** Test section
- Figure 3.5** Diffuser
- Figure 3.6** Suction chamber
- Figure 3.7** Test section (picture)
- Figure 3.8** Thermocouple arrangement for heated plate
- Figure 4.1** Nusselt No. Versus Rayleigh No.
- Figure 4.2** Heat Flux versus Plate Spacing

Figure 4.3 Nusselt No. Versus Plate Spacing for different static Pressures ($T_s = 50^\circ\text{C}$)

Figure 4.4 Nusselt No. Versus Plate Spacing for different static Pressures ($T_s = 60^\circ\text{C}$)

Figure 4.5 Nusselt No. Versus Plate Spacing for different static Pressures ($T_s = 70^\circ\text{C}$)

Figure 4.6 Heat Flux Versus Plate Spacing for different static Pressures ($T_s = 50^\circ\text{C}$)

Figure 4.7 Heat Flux versus Plate Spacing for different static Pressures ($T_s = 60^\circ\text{C}$)

Figure 4.8 Heat Flux Versus Plate Spacing for different static Pressures ($T_s = 70^\circ\text{C}$)

Figure 4.9 Optimum Spacing versus Static Pressures for different Plate Surface Temps.

Figure 4.10 Optimum Heat Flux versus Static Pressures for different Plate Surface Temps.

Chapter1

GENERAL BACKGROUND

1.1 Introduction

Electronic cooling problems have always been formidable for thermal engineers with respect to their solutions and verifications. This difficulty can be attributed to the presence of composite material with different thermal conductivities and multiple heat sources with different intensities.

In electronic cooling the objective is to ensure that component junction temperature meets the design specification (80° - 100° C) and cooling system is effective enough to provide error free operations for worst possible environment. In other words, electronic cooling is meant for ensuring reliable operation under temperature change. Electronic cooling application areas include PCB's, IC packages, T.V.sets, Digital multimeters etc.

Miniaturization of electronic components has resulted in complex circuits and highly dense electronic boards characterized by high rate of heat dissipation per unit of component area. Heat flux in modern electronic devices can be of the order of about 100 W/cm^2 . This requires an efficient cooling system with high heat dissipative capability. Figures 1.1a,b&c show a typical electronic enclosure with its components.

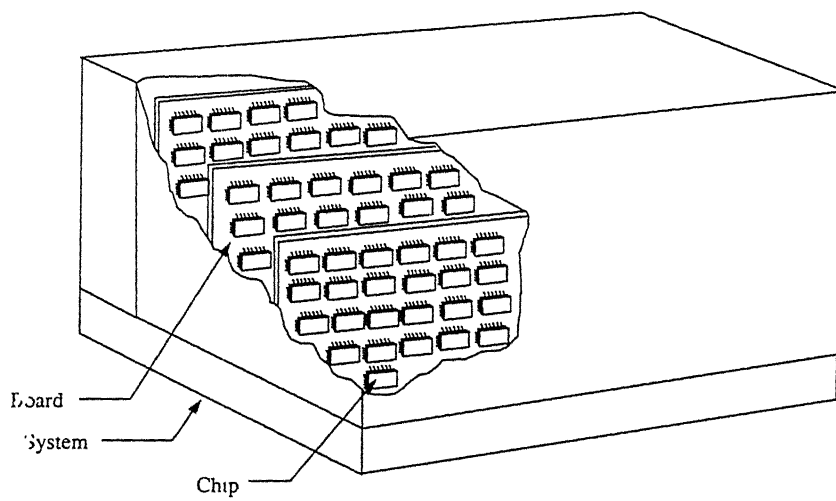


Figure 1.1a: Electronic enclosure

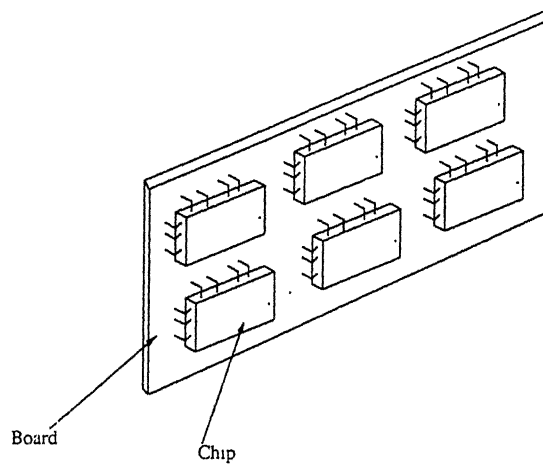


Figure1.1b: Chips mounted on the board

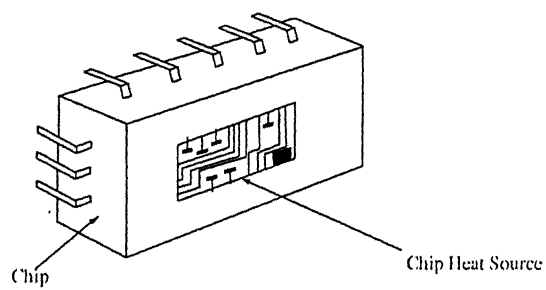


Figure1.1c: Heat generating chip

1.2 Effects of Temperature Rise and Failure Modes

It is important to know why temperature and its reduction are important in electronic systems. Temperature induced stresses are of common knowledge. This could be very well described by fuse burnout case. The fuse bulb can not dissipate the excess heat brought about by the power change. Here thermally induced stresses cause the mechanical failure, as there is no scope for expansion. Thermally induced stresses occur in electronic components when they can not be cooled adequately, resulting in eventual failure. From operational point of view, temperature plays an important role (sensitivity of silicon based devices to temperature is a known phenomenon). The switching voltage response is highly temperature dependent. Large temperature variation at chip level will increase the range over which switching occurs leading to switching errors.

Temperature induced failures are classified as follows:

- (a) Immediate destruction failures.
- (b) Increase in the rate of random failures one time(long term reliability)
- (c) Operational failure at high temperature.
- (d) Intermittent operational failures at high temperature (parts pf the circuit do not work together).

Reduction of the temperature at the device level also reduces stress in the component internal structure. Temperature also plays a significant role in other failure mechanisms that govern the reliability of the component. This can be very well

depicted by looking at the activation energy and its relation to temperature as described by the Arrhenius equation can very well depict this:

$$A_T = EXP \left[\frac{E_a}{K_B} \left(\frac{1}{T_1} - \frac{1}{T_2} \right) \right]$$

Above equation shows an exponential dependence of activation energy (signifying failure rate) on temperature.

1.3 Heat Transfer in Printed Circuit Boards

The thermal transport is described by coupling between components and system parts. To understand electronic cooling, it is important to know about the generation of heat, spreading and eventual departure at component level. This gives us an idea as to how the heat gets transferred from the component to the fluid which is an eventual sink for the fluid (gas or liquid) cooled system.

The generated heat at the chip gets transported through any available path with the bulk being transferred through the least resistant one. The sink where heat is eventually transferred is cooling fluid. The paths available for heat flow are through molding material and the leads. Each material regardless of its thickness impedes the flow of heat as it travels from sources to the sinks. The wire bond also provides another avenue for transport of heat. This can become a major path as the cross sectional area is proportionally large (typical wire bond diameter is 5 μ m).

As soon as heat reaches the leads, part of it is conducted to the board as rest is either convected or radiated to the ambient. Combination of multiple heat sources and different possible paths for heat flow creates complex and non-uniform temperature

fields. Figures 1.2a and 1.2b show various heat transfers mechanisms and their paths followed in a typical PCB.

1.4 Electronic Cooling Methods

Typical electronic cooling methods adopted for heat transfer are as follow:

(a) Natural Convection Cooling

Natural or free convection plays a very important role in cooling of electronic equipments. In this type of convection cooling, temperature difference in the fluid produce density gradients. As a result buoyancy effects drive movement of fluid.

Natural convection cooling is often used in situations where there is low power dissipation or higher temperatures can be allowed. Normally heat transfer coefficient achievable in natural convection is of the order of $5 - 25 \text{ W/m}^2 \text{ K}$. This limits the heat flux to a value of $0.1 - 1.0 \text{ W/cm}^2$ and allowable temperature to less than 100°C . Despite significantly lower surface heat transfer coefficient natural convection is preferred for low end equipments, compared to forced convection or immersion boiling, because of its inherent reliability and simplicity.

Electronic test equipments, consumer electronics, low-end computer packages and communication switches are often cooled by natural convection.

(b) Forced Convection cooling

In forced convection the fluid movement is due to some external action such as a fan or pump. This type of cooling method is used for higher power dissipation levels or in applications such as the space shuttle where near zero gravity eliminates buoyancy

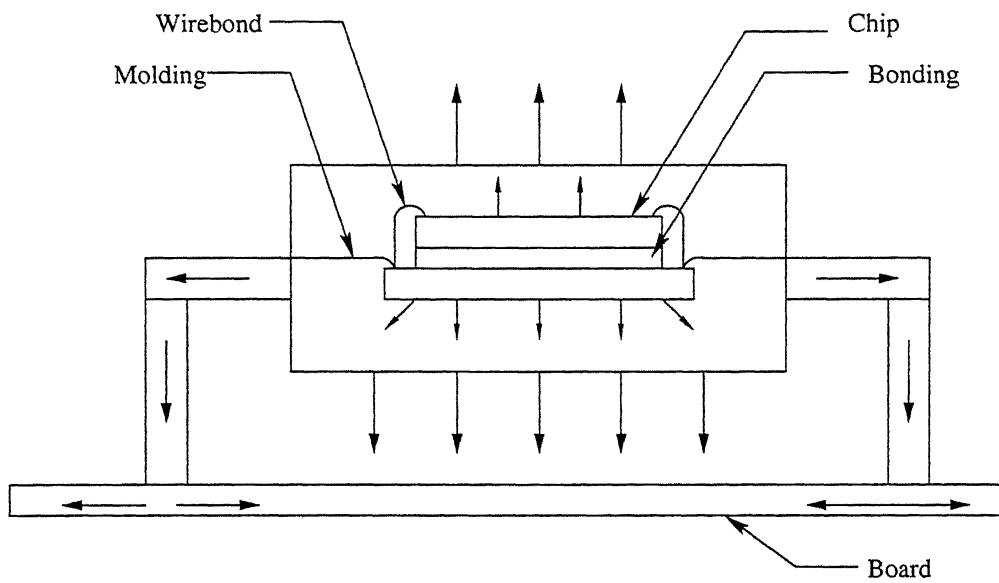


Figure1.2a: Heat transfer in an electronic component

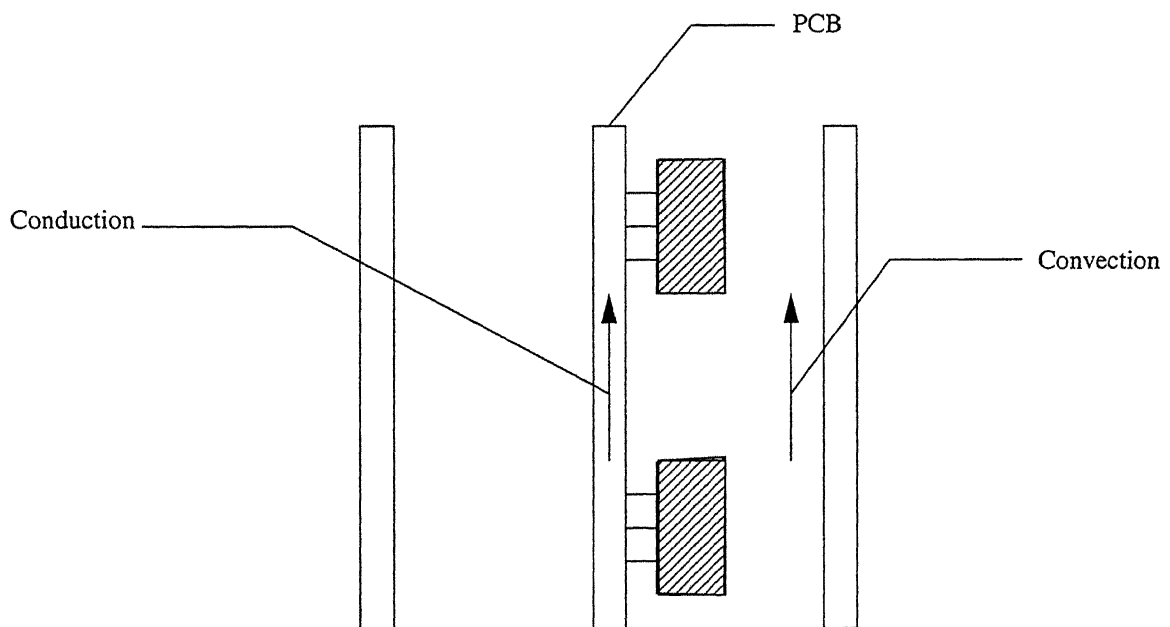


Figure1.2b: Paths of heat transfer

driven flow. Experiments show that forced convection can enhance heat transfer by 10 times as compared to natural convection. High heat dissipation leads to increase in costs, noise, power consumption and complexity. Forced convection has led to significant advances in the performance of indirect cooling schemes such as micro channel cooling. Typical micro channel with air results in thermal resistance as low as 0.75°C/W , which can be achieved for airflow velocity of 37m/s .

Forced convection cooling is commonly used for electronic systems with high-speed memory chips, multi chip modules etc and other large heat generating circuit elements.

(c) Mixed Convection Cooling

Mixed convection is defined as a heat transfer situation where both natural convection and forced convection heat transfer mechanisms interact. In a vertical passage, the internal main flow can be characterized in two ways:

(1) Buoyancy assisted (Upward Flow)

(2) Buoyancy opposed (Downward Flow)

In buoyancy assisted flow, natural convection created by buoyancy is in the same direction as the bulk flow. In contrast, the downward flow is based on its direction opposite to the natural convection. Regardless of the type of convection, the heat transfer is always between the vertical plate and the fluid reservoir between them. Non dimensional parameter that determines the type of convection dominating is given as follows:

$$\frac{Bo_y^{1/4}}{Pe_y^{1/2}} \begin{cases} > O(1), & \text{Natural - convection} \\ \approx O(1), & \text{Mixed - convection} \\ < O(1), & \text{Forced - convection} \end{cases}$$

In past few years mixed convection in a heated channel has received considerable attention due to its extensive practical applications, such applications include house hold electronic devices and equipments, industrial electronic packages, large mainframe systems, avionics and space electronics, nuclear reactor electronic components and so on. Here in all cases, the target is to optimize the power consumption and heat flux dissipation as well. It is found that enhancement of heat transfer is most pronounced when the channel is horizontal and heat transfer is taking place from the bottom surface, yet in electronic devices vertical plate stacking is preferred because of space limitations to allow heat to be conducted from both sides.

1.5 Methodology for designing a cooling system

From simplicity point of view, we consider a single chip module residing on a board and air is flowing over the component for the purpose of maintaining its junction temperature below the design specification. The objective here is to obtain the junction temperature of the component, which is a function of the board thermal conductivity, component surface and fluid temperatures. The methodology adopted here is shown in the following figure1.3.

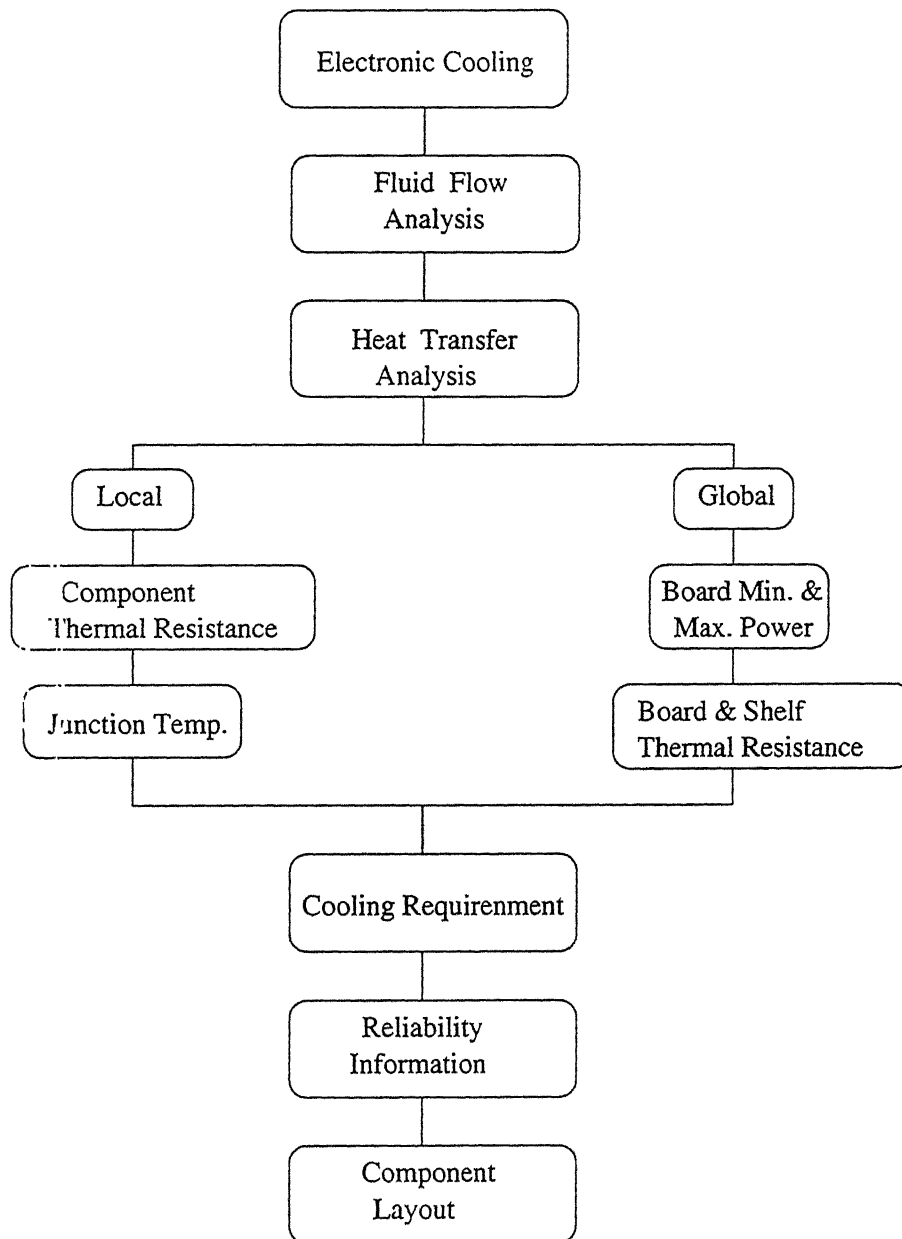


Figure 1.3: Flow chart for Cooling of a PCB

Chapter 2

LITERATURE SURVEY

2.1 Introduction

This chapter is a brief account of works done in the area of electronic cooling. This includes the summary of analytical, numerical and experimental works reported in literature. This literature survey is not only to facilitate the improvement of existing schemes but also to provide a basis for development of new ones. The survey is not only limited to the investigation performed over the last few years, but it also covers some of the landmark works done over the few decades as well. It includes information on possible simulation of fluid flow and heat transfer processes specifically related to the thermal control of the semiconductor devices, modules and the complete systems.

Various research efforts done in this field comprise of the following heat transfer

mechanisms.

1. Natural Convection.
 2. Forced Convection.
 3. Mixed Convection.
 4. Phase change.
 5. Jet Impingement.
- Each of the mechanisms have been explored experimentally, analytically and also numerically.

This chapter deals with mixed convection only and therefore works done in this area only are summarized.

2.2 ANALYTICAL STUDIES

Min-Joon et al. [1] investigated one dimensional mixed convection of liquid metal with forced circulation and unequal heating. The steady solutions of the corresponding heat equations with proper boundary conditions were obtained analytically. The solutions showed formation of local circulation loop by unequal heating and deformation of the circulation loop by the forced convection. It was also found that the heat transfer characteristics were almost independent of the unequal heating conditions although the deformation occurred more easily for a more symmetric case.

2.3 EXPERIMENTAL STUDIES

Tewari and Jaluria [2] carried out an experimental study on the fundamental aspects of

the conjugate, mixed convective heat transfer from the finite width heat sources which were of negligible thickness and had uniform heat flux input at the surface. These were located on a horizontally or vertically oriented flat plate. Two dimensional flow circumstances were simulated and the convective heat transfer mechanism was studied in detail by measuring surface temperature and determining the heat transfer coefficient for two heated strips representing isothermal sources. Results obtained have great relevance in cooling of electronic systems. Results showed sharp variations in the surface temperatures near the leading and trailing edges of the heated stripes for both horizontal and vertical surface orientations. It was also found that in the horizontal orientation of the surface even a strong heat source has a negligible effect on the surface temperature of relatively weak neighbouring heat source. This was attributed to the insignificant interaction between vertical rising wakes from the two heat sources. Schematic of the setup used is shown in figure 2.1.

Chen et al. [3] investigated the linear stability analysis of mixed convection in a differentially heated vertical channel for Prandtl number values of 0.7, 7.0, 100, and 1000. The viscous flow investigated in this paper was the mixed convection, which was driven by an external pressure gradient and also by a buoyancy force, between the two parallel long vertical plates separated by a distance. The gravitational force was aligned in the negative x-direction. There was a fixed temperature difference, produced by maintaining the two vertical walls at different temperatures T_1 and T_2 respectively. It was found that both the Prandtl number and the Reynolds number were important parameters in determining the critical Grashoff number Gr_c , critical wave number α_c ,

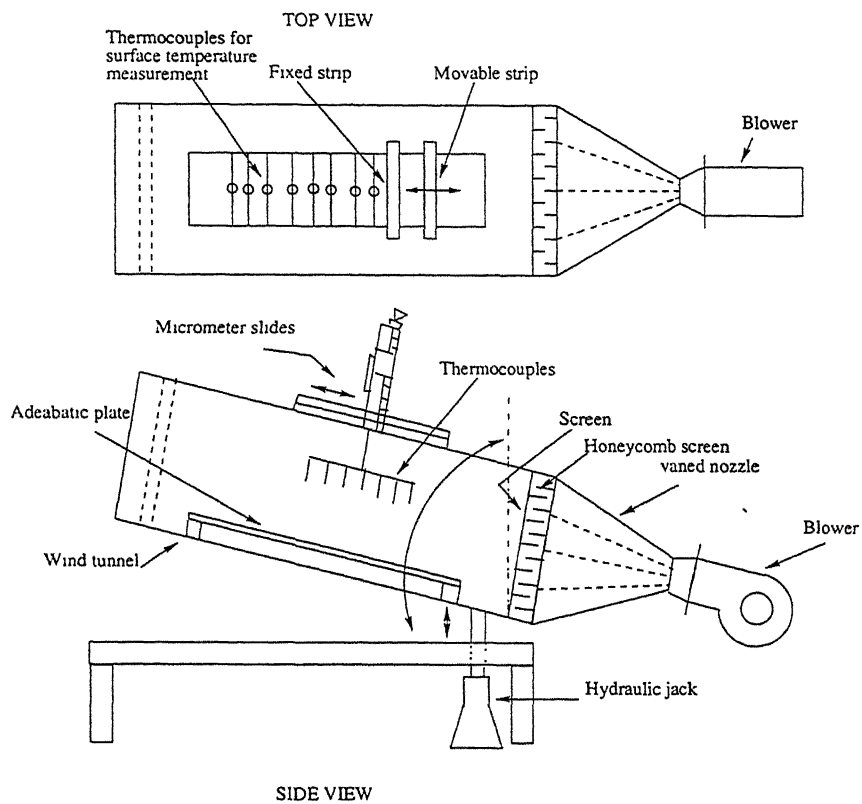


Figure 2.1: Schematic of the test rig used by Tiwari and Jaluria

wave speed C_r and instability mechanism for higher Prandtl numbers. For the lower Prandtl numbers, the effects of the Prandtl number and the Reynolds number were relatively small. The most significant finding was that the local minimum wave number was 8.0 for $Pr=1000.0$, which was substantially higher than those found before for earlier heated flows. In general, for mixed convection channel flows, the instability characteristics of the differentially heated flows were found to be substantially different from those of uniformly heated flows. For constant heat flux case, instability type was in general Thermal buoyant instability for the buoyancy assisted flow. In case of constant wall temperature, thermal shear instability was generally found for low to moderate Reynolds numbers.

Tso et al. [4] measured convective heat transfer from a linear array of flush mounted heat source in a vertical flow up channel. Water was used to simulate the dielectric fluid. The dimensions of the simulated chips were held constant while height of the channel was varied. The experiments were conducted in a closed-loop liquid cooling flow facility, with a vertical up-flow, in a plexiglas test section. The first chip was located 680.0 mm downstream of the channel inlet. providing a minimum hydrodynamic entry length of 50 hydraulic diameters. Channel height was varied over values of 0.5, 0.7, 1.0 times the heated source length. The heat flux was set at three values of 0.5, 10.0 and 20.0 W/cm^2 . Reynolds number based on heat source length ranged from 6×10^2 to 8×10^4 . The results obtained agree well with the results for air-cooling of heated sources of similar geometry when Peclet numbers were used to correlate the data in the laminar flow and the Nusselt numbers were normalized against the

Prandtl numbers in the turbulent flow. They suggested that data from air cooling might be used to predict the heat transfer characteristics of the liquid cooling of a similar geometry if the Prandtl number scaling was considered.

Tseng et al. [5] carried out an experimental investigation combining flow visualisation and temperature requirements to unravel the effect of tapering the top plate of the rectangular duct about the detailed changes in the vortex flow structure in a mixed convection air flow through a bottom heated trapezoidal duct. Special care was taken on the flow stabilization and the weakening of the vortex flow by the acceleration of the primary flow for the various Reynolds and Grashof numbers. The spanwise-averaged Nusselt numbers for the horizontal rectangular and tapering ducts were obtained to further detect the temporal stability of the flow. Over the ranges of the Re and Gr investigated for $5 \leq Re \leq 102$ and $1.0 \times 10^4 \leq Gr \leq 1.7 \times 10^5$, the vortex flow induced in the rectangular duct exhibited temporal transition from a steady laminar to the time periodic and then to chaotic state at increasing buoyancy to inertia ratio. During the course of the study it was realized that although the top plate tapering resulted in the complete stabilization of the vortex flow, the weaker vortices still dominated the secondary flow in the tapering duct.

Zhang et al. [6] conducted experiments and analysis of buoyancy-assisted mixed convection in a vertical square channel with asymmetric heating conditions. Most published literatures in mixed convection are based on test geometry with all sides heated. This work was an assisted mixed convection in a vertical square channel under four symmetric heating conditions i.e. with one or two sides heated. This created a

stronger three dimensional flow disturbance that could change heat flow characteristics both upstream and downstream. The paper covers the laminar, transition, fully turbulent flow regimes. The Reynolds number was varied from 200 to 11200 and the buoyancy parameter, $\frac{Gr}{Re^2}$, was varied from 0.02 to 200. It was found that local heat transfer coefficient increased with the increasing buoyancy parameter. The Nusselt number ratio, $\frac{Nu}{Nu_o}$ was observed to increase significantly with the increased turbulent mixing caused by more irregular heating conditions. The increase in the coefficient could be attributed to three-dimensional large scale buoyancy- induced motion in the flow field.

Ligrani et al. [7] investigated mixed convection in straight and curved channels when buoyant forces were perpendicular to the bulk flow direction. Grashof number based on the temperature difference ranged from 0 to 50×10^6 , and the Reynolds number based on channel width ranged from 343 to 2057 which gave laminar and transition forced flow. The flow behaviour was classified into four different regimes viz,

1. pure natural convection,
2. mixed convection with strong buoyancy,
3. mixed convection with weak buoyancy, and
4. pure forced convection.

The authors discussed the difference in the behaviour between these different regimes along with the curvature influences and suggested Nusselt number correlations for the two mixed convection regimes. Test rig used for the purpose is shown in figure 2.2.

Gau et al. [8] conducted an experimental study of the mixed convection in a heated

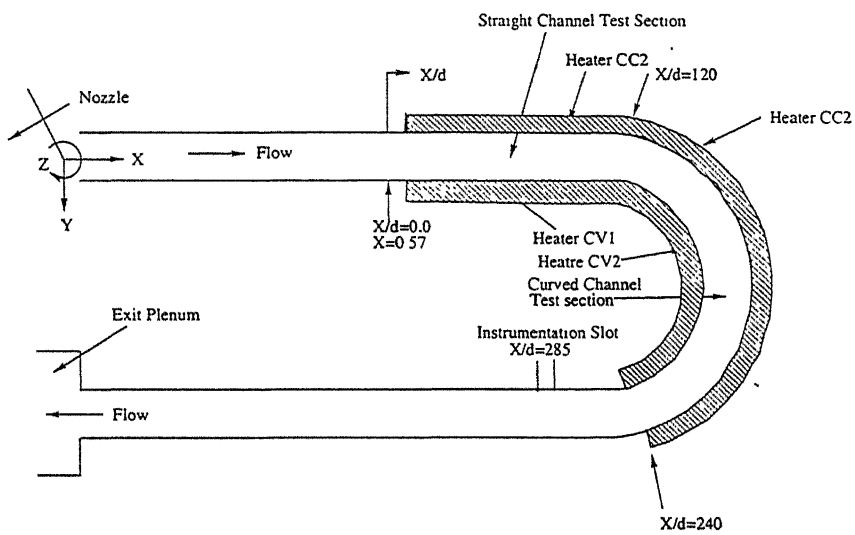


Figure 2.2: Ligriani's setup for mixed convection in straight and curved channels

divergent channel with one wall held in the vertical position. The vertical wall was heated uniformly while, the opposite wall, which had a divergent angle of 3.0 degree was tilted away from heated wall and was well insulated. They studied the occurrence and the structure of the reversed flow and the heat transfer in a heated vertical divergent channel. For the purpose of comparison, results for the parallel plate channel were also presented and discussed. The Reynolds number for the main forced flow ranged from 100 to 4000 and the buoyancy parameter, $\frac{Gr}{Re^2}$, varied from 0.3 to 907. Flow reversal was found for assisted and opposed convection. It was found that the divergence of the channel decelerated the main stream such that flow reversed at a much lower buoyancy parameter. The adverse pressure gradient tended to push the reversed flow upstream and led to a deeper penetration of the reversed flow into the channel. The destabilization effect of the divergent channel could lead to breakdown of vortices and transition to turbulent flow. This could significantly enhance the heat transfer. Temperature fluctuation measurements at different locations were used to indicate oscillations and fluctuations of the reversed flow. The effect of the buoyancy parameter on the Nusselt number and the reversed flow structure was discussed. It was found that for the buoyancy assisted convection Nusselt number increased with the buoyancy parameter. For opposed convection the increase in Nu with the buoyancy parameter was related to the occurrence of reversed flow which interacted strongly with the mainstream. The average Nusselt number was determined and correlated in terms of relevant nondimensional parameters for pure, forced and mixed convection respectively. The fluid velocity in the channel was measured with a TSI hot-wire

anemometer using an improved calibration system.

Maughan et al. [9] investigated heat transfer enhancement in a mixed convection flow between parallel plates heated uniformly from below. They performed both the experimental and numerical study. Flow visualization and heat transfer measurements for air flow in a horizontal channel were performed over a wide range of conditions to delineate the regions of forced and mixed convection. The onset of secondary flow was found to precede appreciable heat transfer enhancement. Except for large values of $\frac{Gr^*}{Re^2}$, Nusselt number prior to the onset of enhancement could be predicted with forced convection correlations. Their numerical computations showed heat transfer enhancement prior to the onset of thermal instability in a horizontal channel due to fluid expansion and an induced pressure gradient, and in an inclined channel due to component of gravity in the flow direction. In the numerical work, the plate conduction effects were neglected, and the thermal entry region was investigated by prescribing laminar fully developed flow at the start of the heated section. Assuming steady two dimensional laminar flow and constant properties and the Bousinesq approximation, the appropriate governing equations were non-dimensionalized. The experiments were performed using the horizontal air channel which along with other accessories is shown in figure 2.3.

Ambient air was drawn into blower, metered and conditioned before passing through the channel. Warm air leaving the blower was cooled to ambient temperature with a compact air to water heat exchanger. The inlet temperature of water was controlled by a data acquisition computer which based upon the inputs provided by the ther-

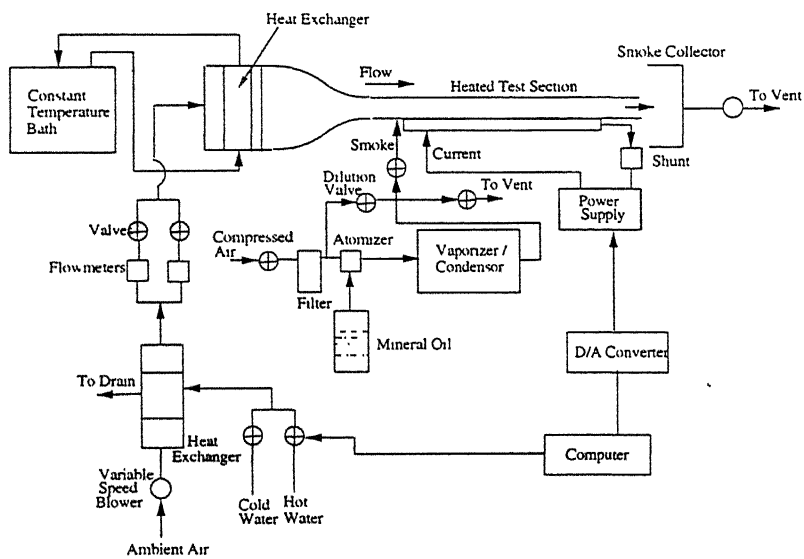


Figure 2.3: Schematic of test rig used by Maughan

thermocouples in the air stream leaving the exchanger, opened or closed an electronically controlled valve mixing hot and cold water. A uniform and constant inlet temperature was assured with additional heat exchanger located just prior to the channel entrance. This exchanger was driven by a constant temperature bath held at the ambient temperature.

Maughan et al. [10] performed few experiments to investigate mixed convection heat transfer in the thermal entry region of a parallel plate channel heated uniformly from below. The effect of surface heat flux and the channel orientation on the local Nusselt number was studied for $Pr=0.7$, $125 < Re < 500$, $7 \times 10^3 < Gr^* < 10^6$, and $0 < \theta < 30^\circ$. Heat transfer initially was dominated by forced convection and showed a rapid decline in the Nusselt number. Following the onset of thermal instability, secondary flow development caused a sharp increase in the Nusselt number, which was followed by maximum subsequent oscillations. The Nusselt number oscillations eventually decayed, yielding a fully developed value which depended on the Grashof number. The onset of instability was delayed by decreasing the Grashof number and/or by increasing the Reynolds number and the inclination angle. For the inclined channel, significant heat transfer enhancement occurred prior to onset of the secondary flow. The experimental test rig used is shown in the figure 2.4.

Ramchandran et al. [11] conducted measurements and prediction of laminar mixed, forced and free convection air flow adjacent to an isothermally heated vertical flat surface. Their experimental test rig is shown in figure 2.5. It basically consisted of low turbulence open circuit wind tunnel which could be rotated and fixed at any desired

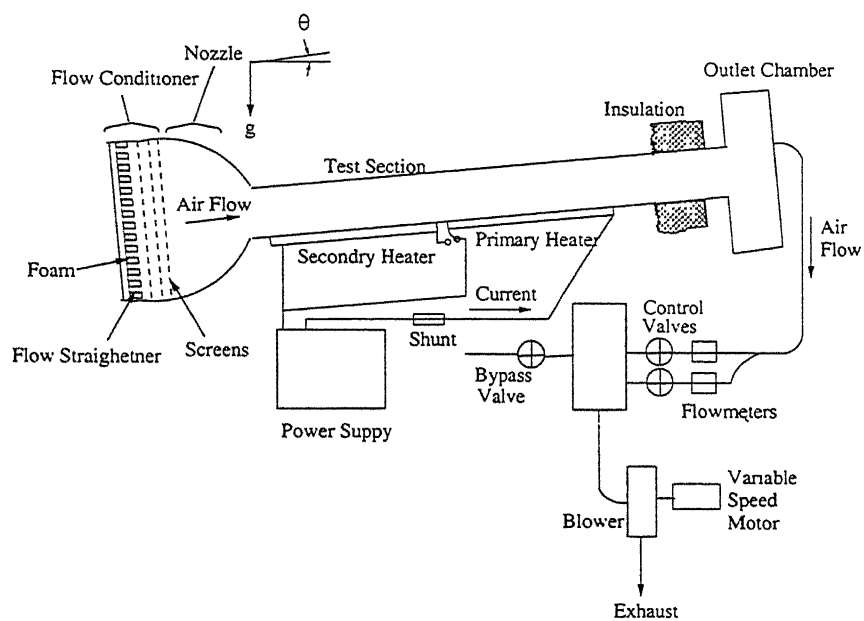


Figure 2.4: Schematic of previous setup used by Maughan

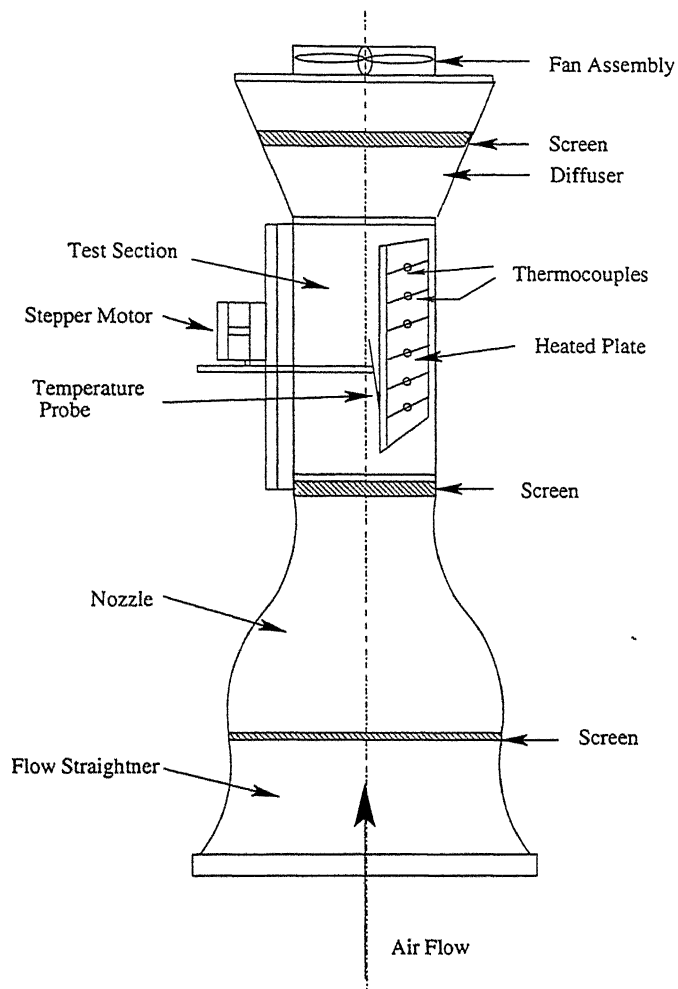


Figure 2.5: Schematic of setup used by Ramchandran to study laminar mixed, forced and free convection

inclination angle. The tunnel had a smooth converging nozzle with a contraction angle ratio of 9:1, a straight test section and a smooth diverging diffuser. Plastic honeycomb material (10.00 cm thick) and several wire screens were used in the front section of the tunnel and along the nozzle length and diffuser to straighten the flow and reduce the turbulence level in the test section. The heated flat plate consisted four layers which were held together by screws and instruments to provide an isothermal heated test surface. In this study local Nusselt numbers and the velocity and temperature distributions were presented for both the buoyancy assisting and opposing flow cases over the entire mixed convection regime, from pure forced convection limit (buoyancy parameter $\xi = \frac{Gr_x}{Re^2} = 0$) to the pure free convection limit ($\xi = \inf$). It was found that the mixed convection Nusselt numbers were larger than the corresponding pure forced and pure free convection limits for buoyancy assisted flow and were smaller than these limits for the opposing flow. Flow reversal near the wall was detected for buoyancy opposing flow case at a buoyancy parameter of about $\xi = 0.20$.

Yadav et al.[12] conducted an experiment to determine heat transfer characteristics of a stack of vertical heated plates. The geometrical configuration designed and fabricated for this work simulated the printed circuit boards(PCB's) used in various electronic devices. The uniform heat flux model was adopted. Heat flux from the plates was kept every time at a value such that temperature at any point shall not exceed the preferred temperature limit. It was shown that heat transfer rate could not be enhanced indefinitely by increasing the coolant driving pressure. Certain points were identified on the plate surfaces where high heat flux could be safely reached.

Several other noticeable trends were observed regarding power consumption etc.

2.4 NUMERICAL STUDIES

Rao et al.[13] numerically studied a two dimensional steady state conjugate problem with laminar compressible flow in mixed convection with surface radiation from a vertical plate with a flush mounted discrete heat source. The effects of the magnitude and location of the heat source, the material and surface properties of the plate and the free stream velocity on both heat transfer and fluid flow were studied. Vorticity stream function was used to write the governing equations and were finally solved using finite volume based difference method. It was found out that the best position for the heat source was the leading edge of the plate and the least preferable position was the trailing edge, as the latter position increased θ (non dimensional temperature) by 35 - 50 percent for the entire range of R_{il} . For a given $R_{il} = 1$, convection was dominant taking away as much as 90 - 95 percent of heat generated for good reflecting surfaces.

Papanicolaou and Jaluria [14] conducted a numerical study on the combined forced and natural convection air cooling of heat dissipating electronic components located in a rectangular enclosure. Flow and thermal fields in flowing air, at the walls of the enclosure and mounted electronic components were obtained. Results for laminar and oscillatory domains were presented which have vital importance in the search for a suitable placement of electronic components in a given enclosure for effective heat removal.

Davalath and Bayazetogue [15] investigated conjugate heat transfer for two dimen-

sional developing flow over an array of rectangular blocks which represented finite heat sources on parallel plates. Incompressible flow over multiple blocks was modeled using fully elliptic forms of Navier Stokes equations. A control volume based finite difference procedure with appropriate averaging for diffusion coefficient was used to handle coupling between solid and fluid regions. They have extended the analysis to study the optimum spacing for a fixed heat input to achieve desired maximum temperature at the heat source.

Barletta et al. [16] investigated mixed convection of the power-law fluid in a vertical annular duct in a regime of laminar fully developed flow. Uniform and unequal temperature were prescribed on the inner and outer boundary walls. The momentum balance and the energy balance equations as well as the viscous stress constitutive equations were solved analytically in order to obtain the velocity fields, the viscous stress field and the temperature field. The analysis of the cases was done for :

1. Mixed convection of a Newtonian fluid, and
2. Forced convection of the power law fluid given by

$$\tau_{yx} = -m \left| \frac{dv_x}{dy} \right|^{n-1} \frac{dv_x}{dy}$$

for $n = 1$, this equation stands for Newtonian Fluids.

In the first case it was shown that the condition for the onset of the reversed flow implied the existence of a threshold value for $\Lambda = \left| \frac{Gr}{Re} \right|$ which depended on the $\gamma = \frac{R_1}{R_2}$ (ratio of inner to outer radii). When These Threshold values were exceeded, flow reversal occurred next to the inner boundary wall. In the case of mixed convection

for the power law fluids, the flow reversal conditions were investigated. As for the Newtonian fluids, flow reversal occurred when the threshold values of $\text{mod } \lambda$ were exceeded. These threshold values depended on both γ and inverse of power law index (m). Further for the fixed values of γ , Threshold values were increasing function of m . Moukallad et al. [17] numerically studied the mixed convection heat transfer in a channel with heated curved surface bounded by a vertical adiabatic wall. Two cases were considered, in the first case the flow experienced a convex curvature on an increasing cross-sectional flow area (adverse pressure gradient), while in the second case, the flow experienced a concave curvature with a decreasing flow cross-section (favorable pressure gradient). Governing equations were conservation of mass, momentum and energy. Flow was considered to be steady, laminar and two dimensional. The volume approach was adopted to solve numerically the coupled system of equations governing the flow and temperature fields. For the convex entry channel, it was observed that for low (Gr/Re^2), the Nusselt number reached a minimum near the onset of flow separation along the heated wall of the convex-entry channel and then decreased towards the channel exit. The effect of increasing Prandtl number on the total heat transfer was considerably greater than the effect of increasing (Gr/Re^2). For concave-entry channels, the flow separation was not encountered. The decreasing cross-sectional area combined with buoyancy increased the channel velocities near the wall gradients. Therefore, the surface heat transfer rates were considerably greater than in the convex-entry channel. The overall heat transfer in a concave-entry channel was always greater than a straight channel of equal heated surface area, a critical

value for the ratio (Gr/Re^2) existed, below which heat transfer enhancement was obtained with concave-entry channels.

Yadav and Kant [18] developed a theoretical model to numerically simulate mixed convection cooling in a stack of vertical heated plates representing the PCBs. For the given spacing between the plates, they estimated the maximum amount of heat that could possibly be transferred to the coolant at a certain static pressure difference between the top and the bottom of the stack and also the maximum possible heat flux from the surface being cooled. It was shown that the need for the optimum spacing between the plates became more important when the driving pressure reached a relatively high level. The following empirical relation was suggested for predicting the heat flux corresponding to the optimum plate spacing for a given static pressure :

$$Q_f = \log \frac{\Delta P + 45}{10} + \frac{\Delta P^{0.505}}{1000} - 0.205$$

Cheng et al. [19] looked upon the mixed convection in a differentially heated vertical channel for various Prandtl numbers. Galerkin method was used to solve coupled momentum and energy equations along with continuity equation. They predicted that Prandtl and Reynolds numbers had very important effect on the Grashof number, wave number, wave speed, instability mechanism for higher Prandtl numbers. It was found that the local minimum wave numbers were as high as 8 for $Pr=100$, which was substantially higher than those found earlier for other heated flows.

2.5 CLOSURE

Research efforts in the area of cooling of electronic components have used several heat transfer mechanisms as mentioned in the text. Mixed convection happens to be most

common and convenient due to certain merits. Due to the miniaturization of electronic components, heat dissipation rates per unit area are quite large and the efforts are being made to increase it even more by using one or a combination of mechanisms. Lot of work has been done in the field of mixed convection as such. Experimental studies have been made with straight, curved and divergent channels using constant heat flux and constant surface temperature conditions. Buoyancy and pressure driven flows have been studied. But the subdomain of these works relating to the mixed convection cooling in electronic equipments is not very large. The models adopted for these specific studies have been relooked and modified according to the recent needs. Selected works pertaining to the electronic cooling were presented as briefly as possible without distorting the essence of the original work. Going through the presented material one can realize the need of target oriented research work i.e., the modelling of printed circuit boards and their possible configurations inside the cabinet etc.

Chapter 3

PROBLEM DESCRIPTION AND EXPERIMENTAL SET-UP

3.1 Introduction

As already discussed, mixed convection cooling has a clear edge over natural convection and forced convection cooling methods. It possesses the simplicity and less noisy features of natural convection simultaneously having high heat removal capability of forced convection. In order to simulate a mixed convection cooling problem one has to take into consideration various parameters that go into making of an actual heat generating source in today's PCB's. Some of them are like the alignment of heating element, its location with respect to the cooling system and cooling fluid, type of cooling fluid used and so on. For such a complex problem like the present one, it becomes necessary to follow a systematic approach and make assumptions wherever necessary.

3.2 Experimental Requirements

In order to conduct experimental study on the cooling mechanisms inside various electronic equipments and devices, one has to model a PCB along the following lines. As already discussed, there are various parameters which should be taken into account while simulating a true printed circuit board.

- (1) It's possible arrangement.
- (2) It's possible variety of dimensions.
- (3) Possible orientation of a single PCB with respect to other PCBs.
- (4) Variety of possible mounting or arrangements for electronic chips having different temperatures.
- (5) Type of cooling fluid used (air or water).
- (6) Modes of cooling, whether free or forced or combination of both.
- (7) The unit driving the working fluid or static pressure creating device and its location.

But in the current experimental study it is not possible to have all the flexibility of parameters. We shall stick to certain parameters, which satisfy our requirements for obtaining the maximum cooling effects and least power consumption. Looking at the current requirements of electronic cooling following parameters are taken care of:

- (1) Material used must possess the specified thermodynamic properties within the specified temperature range.

- (2) Driving fan must be located at a place from where the acoustic electromagnetic disturbances shall have minimum effect, as it can affect badly the sensitive components mounted inside.
- (3) Working fluid must move within the specified limits as turbulence may lead to damage.
- (4) There should be provision for air filters to remove unwanted dust particles, which could prove to be damaging agents for delicate components and may choke the micro passages for coolant entry.

3.3 Objectives

The objectives set for the present study were as follows:

- (1) Design and development of an experimental apparatus for Simulation of Mixed Convection Cooling of PCB type configurations.
- (2) Make a parametric study of the variables involved e.g. inter plate spacing and static pressure to determine Convective heat transfer coefficient, average and maximum heat flux.
- (3) Suggest suitable correlation among the variables.

3.4 Experimental Set-up

In the present study mixed convection cooling was simulated experimentally for PCB type configurations. In this experiment one vertical channel formed by two simulated PCBs was placed in the test section where a lead screw mechanism was used for varying the spacing. A suitable static pressure creating device (a fan unit) was provided to suck the air passing through the vertical channel. One of the two plates was acting as an insulating wall while the other consisted of heating elements. There

were five heating elements in the heated plate. Vertical orientation of the channel helped in achieving the mixed convection. Since the suction device was placed at the top of the test section, the buoyancy assisted mixed convection flow was achieved. Completely assembled experimental test setup is shown in figure 3.1. The objectives of the experiment dictated the test rig configuration. It was essential to take into account the accessibility and the flexibility of its components so that there was not much difficulty in taking care of maintenance and repair problems. Provisions for rapid configurational changes were very important and these were incorporated in the design. Figure 3.2 shows the schematic diagram of the test rig designed for the purpose.

Test rig consisted of the following major parts:

- (a) Air intake unit,
- (b) Test section,
- (c) Diffuser unit, and
- (d) Suction chamber (fan unit).

The detailed description as follows:

(a) Air intake unit

This unit helped in achieving smooth entry of air at the test rig inlet. This unit was designed such that the flow at the inlet of test section was fully developed as far as possible. It was basically a converging duct with rectangular cross-section. The dimensions are shown in figure 3.3. The material used for intake unit was galvanized iron sheet. Since few thermocouples were placed at the



Figure 3.1: Experimental Setup

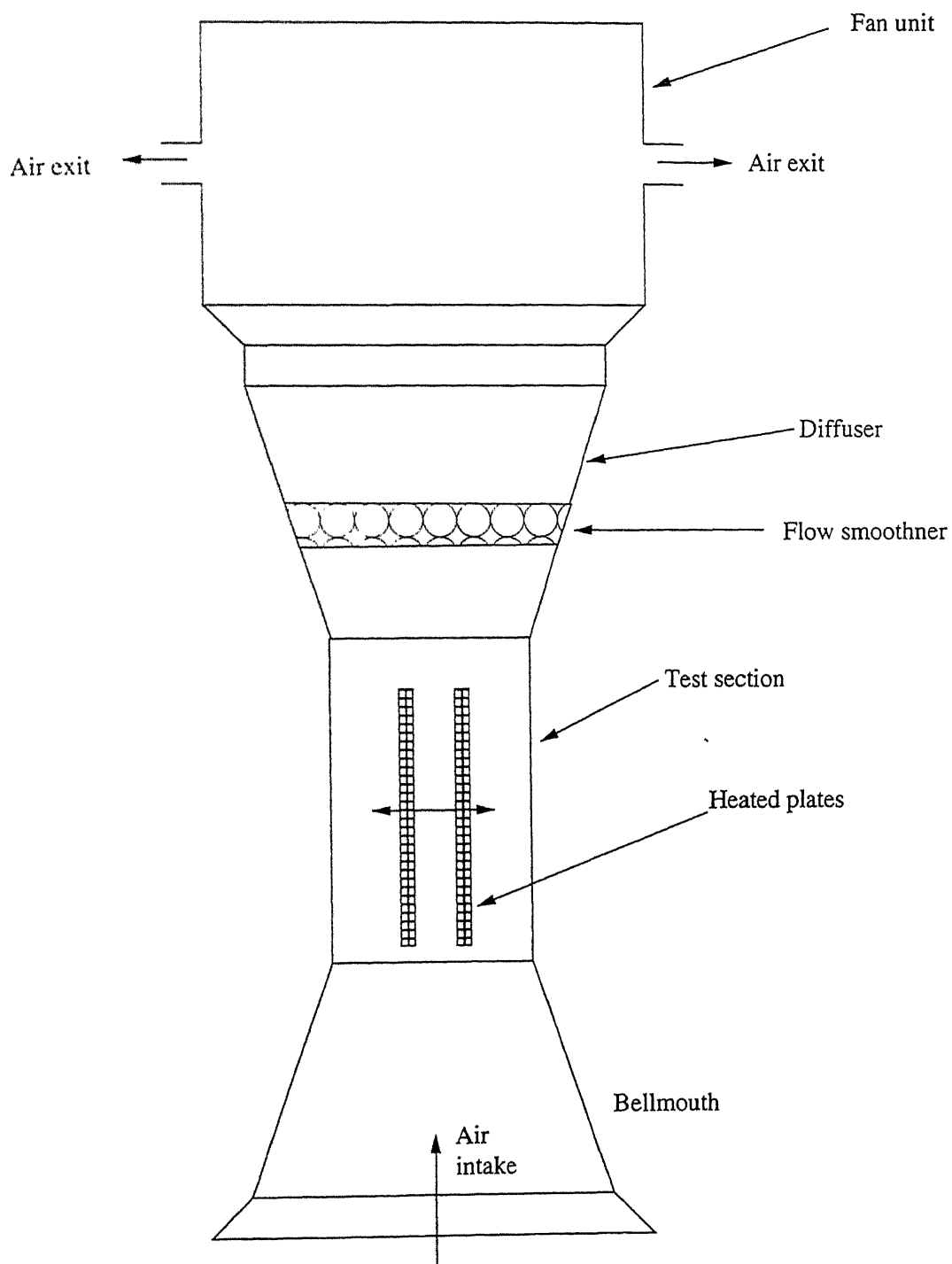


Figure 3.2: Experimental test-rig(Schematic diagram)

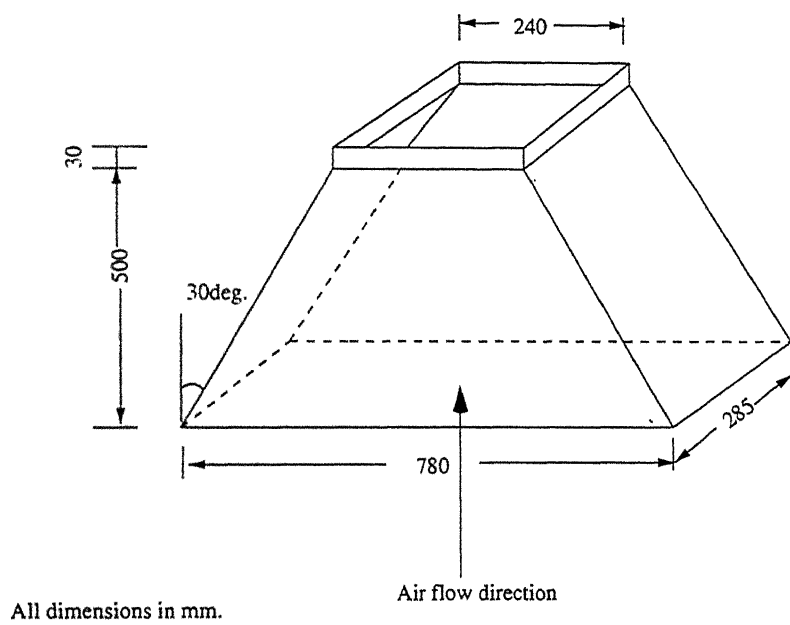


Figure 3.3: Air intake unit

exit of this unit, the metallic sheet helped in eliminating the electrical disturbances due to other electrical appliances used in the lab.

(b) Test section

The cross-sectional area of test section primarily determines overall size of the test section. Test section being the most important part was designed taking into account structural cost, power cost etc. Many shapes for the cross section of test section are used like round, elliptical, square, hexagonal and octagonal with minimal difference in losses due to its shape. But the current study used a square cross section. Length of the test section should be optimized as it affected the power consumption. It should not exceed the required length. Figure 3.4 shows the test section with its actual dimensions. Fifteen-millimeter thick glass plate was used for making the test section. Glass being a good insulator was a right choice for this purpose, it also provided a window for viewing the whole plate assembly.

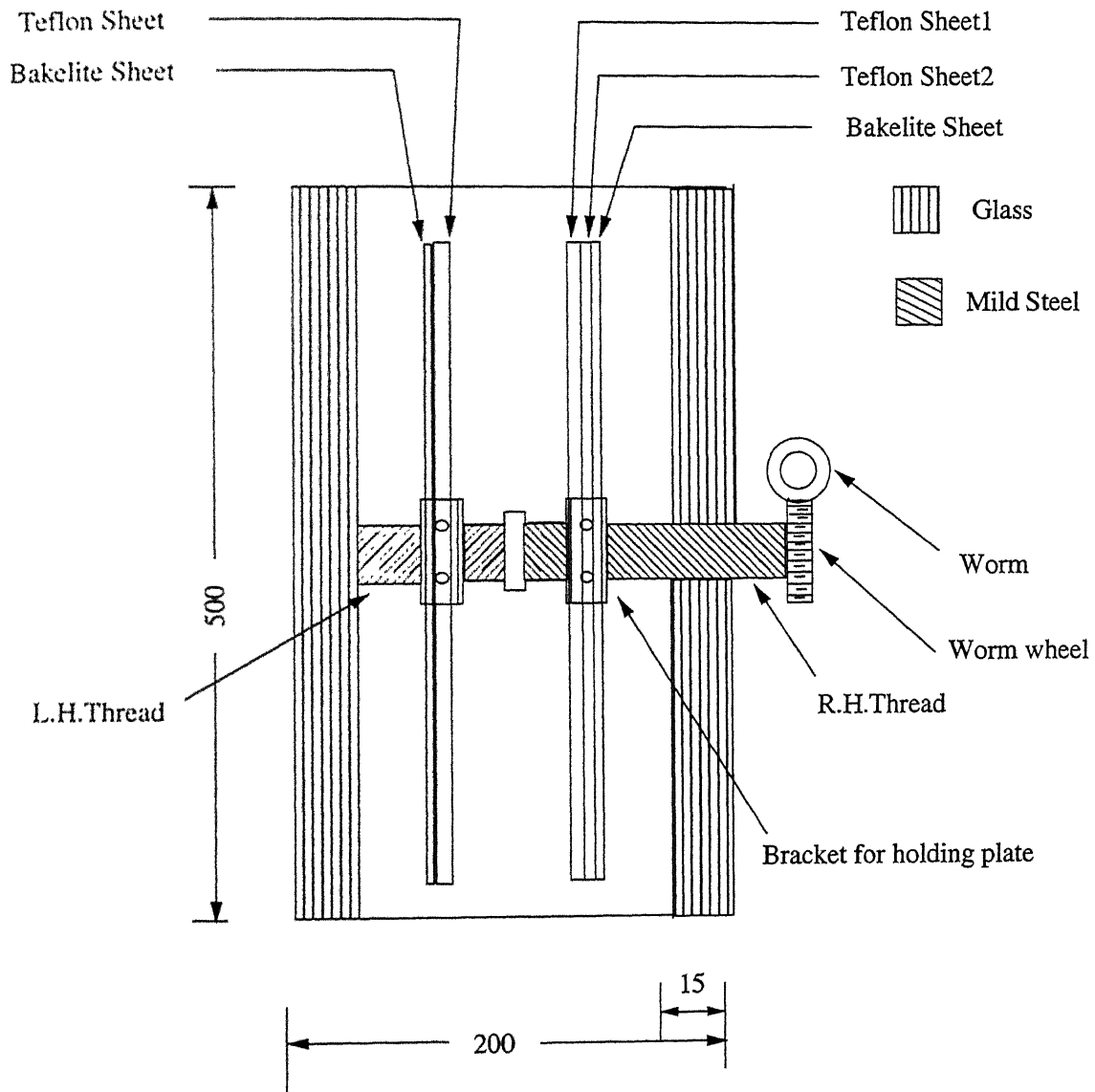
(c) Diffuser

Material chosen for the diffuser was perspex. Figure 3.5 shows detailed dimensional diffuser. Diffuser was designed in order to avoid separation of flow, which would have otherwise led to vibrations, oscillating fan-loading variation in tests section velocities.

(d) Suction Chamber

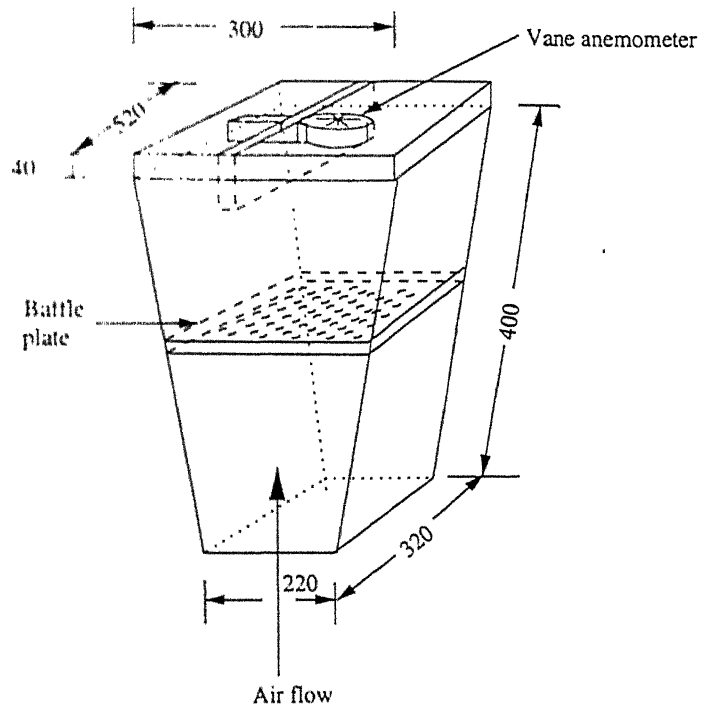
In order to create a pressure differential across the channel, suction chamber was provided with four small fans with the following rating:

Discharge Rate: $0.2 \text{ m}^3/\text{s}$



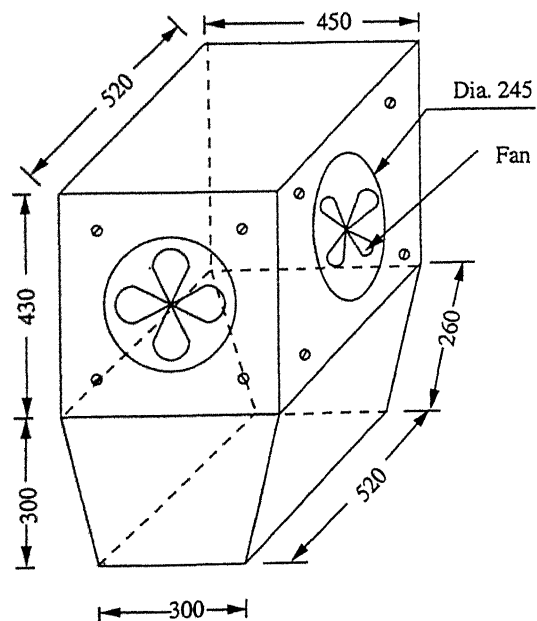
All dimensions in mm.

Figure 3.4: Test section



All dimensions in mm.

Figure 3.5: Diffuser



All dimensions in mm.

Figure 3.6: Suction chamber

Rated Speed: 1440 r.p.m.

The idea behind providing four small fans was to avoid inherent vibration problems in a single fan of large discharge rate. Figure 3.6 shows the dimensional wooden box that was used to house the exhaust fans.

3.4.1 Heated Plates

While designing a heated plate for the simulation of a PCB, following considerations were made:

- (1) The material of the plate was electrically insulating.
- (2) It had the ability to withstand high temperatures (200 -300°C).
- (3) It should be easily machinable.

Looking at the above requirements we have selected Teflon as material for the plate. Its some useful properties are shown in the table 3.1. Complete picture of the plate assembly inside the test section is shown in the Figure3.7. Heating elements with complete details are shown in Figure 3.8. Five such heating elements were placed between the plates.

Teflon Properties

Table 3.1

Melting Point	267 °C
Upper service Temp	150 °C
Tensile Strength	44.5 MPa
Thermal Conductivity	0.2 W/m.K

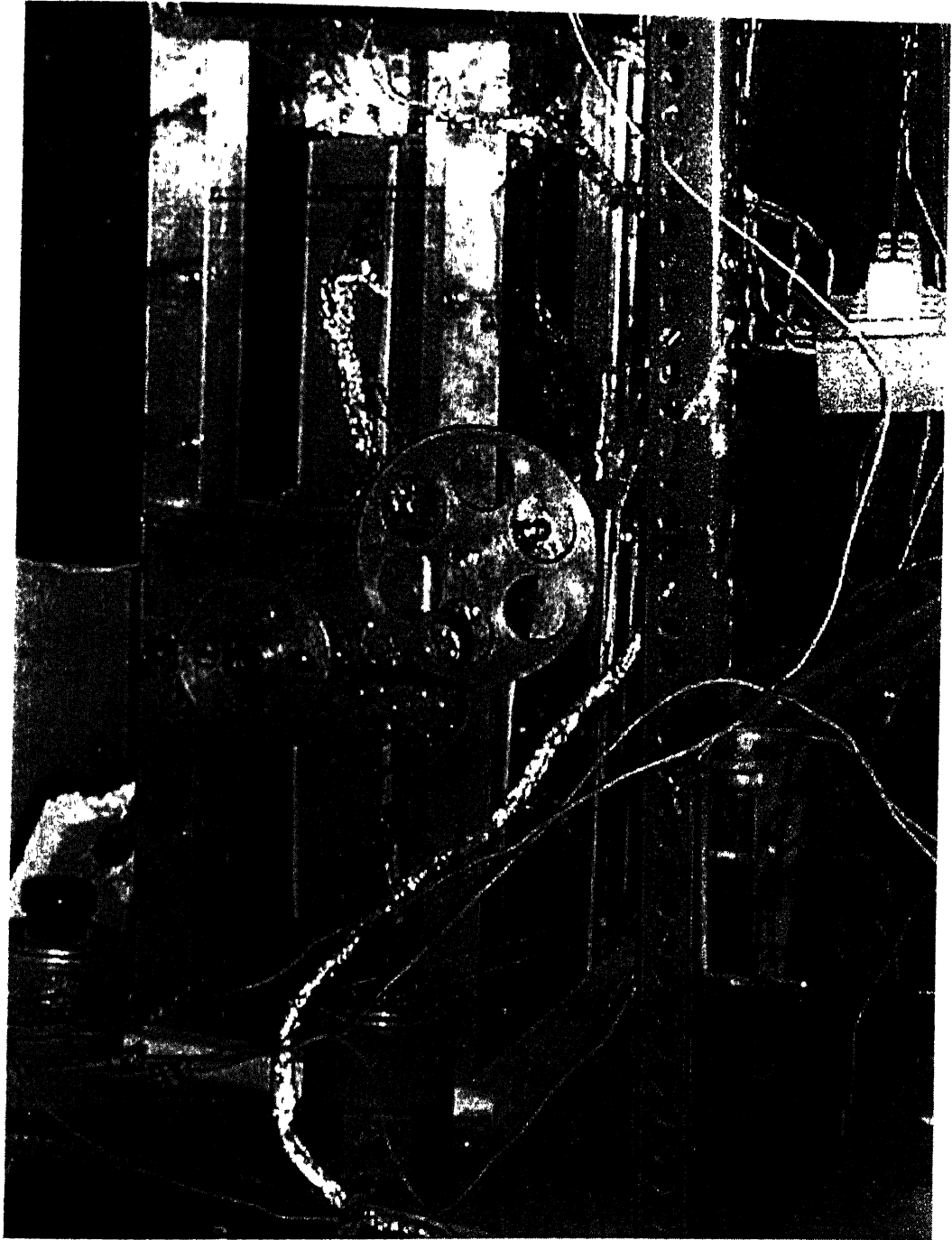
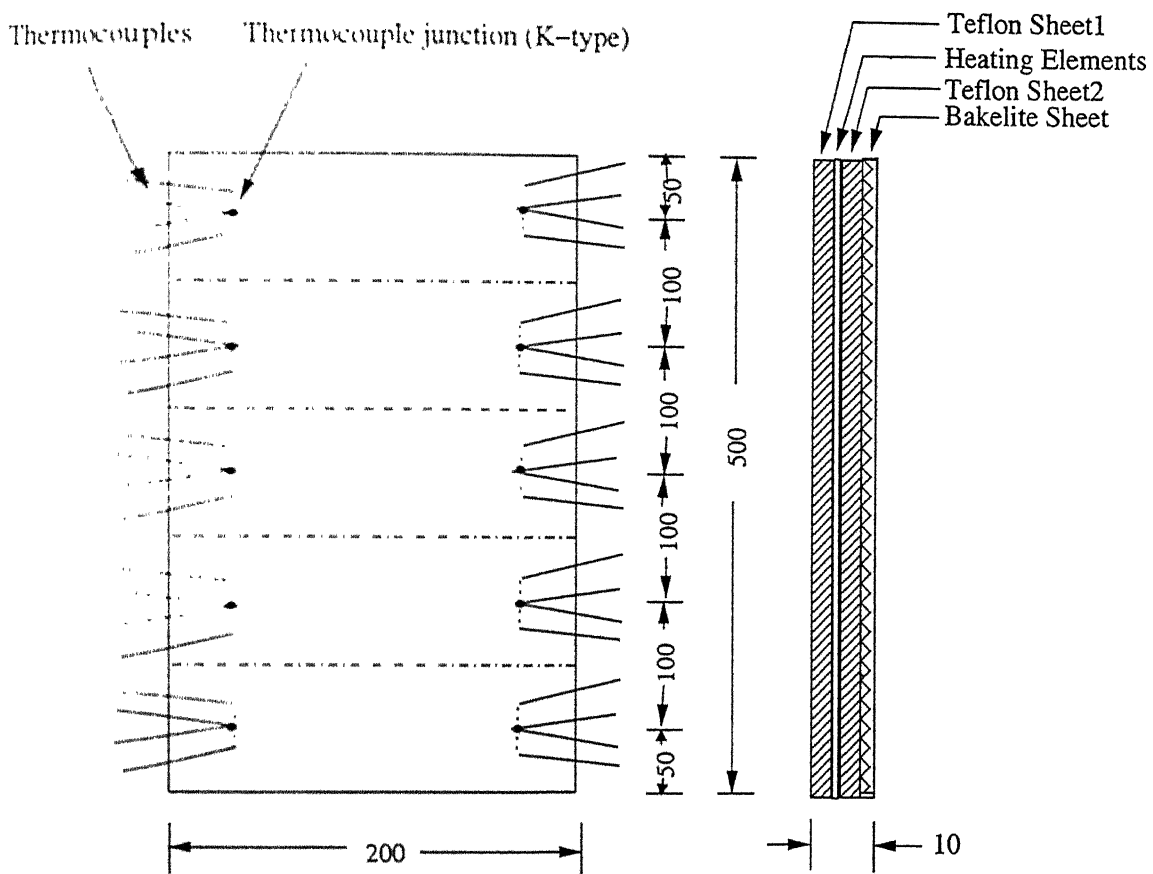


Figure 3.7: Test Section



All dimensions in mm.

Figure 3.8: Thermocouple arrangement for heated plate

3.5 Thermocouple Arrangement

3.5.1 On the plate

For measuring temperature on the plate surface, a total of ten thermocouples were used, two for each section of the plate corresponding to heating elements.

3.5.2 Inside the plate

Additional ten thermocouples were used in a similar fashion to measure the temperature inside the plate assembly. Above temperature measurements were used for finding out heat fluxes from the plates.

In the present work Chromel-alumel thermocouples (K-Type) were used as temperature sensors. These thermocouples were used because of its availability and large temperature range ($-150^{\circ}\text{C} - 1350^{\circ}\text{C}$).

3.6 Experimental Procedure

The experiments were conducted to obtain heat transfer data for a vertical channel formed by a printed circuit board (PCB) like vertical configuration and a thermally insulated wall. For the modeling of a PCB as a plate with uniform surface temperature, different approaches are possible. The approach adopted here can be described as follows.

The entire plate surface was virtually divided into five zones placed vertically one over another. Since the plate height and width chosen were 50 cm and 20 cm respectively, each zone had dimensions of 10 cm \times 20 cm. As the objective was to achieve uniform temperature over the entire plate i.e. same temperature for all the five zones, each zone was heated by a separate strip-heating element. By regulating the

electrical power fed to each element, it was possible to maintain a fixed temperature over each zonal surface and hence (in a sense) over the entire plate, while it was subjected to various cooling rates. As mentioned earlier, four thermocouples were mounted over centerline of each zonal surface, two at the top surface and two beneath it. The difference in the temperature given by each pair was used to calculate the heat flux value for that zone. Further, the pair of thermocouples mounted on the surface of the zone was used to monitor the temperature of the surface and thus regulating the power input to the associated heating element. The uniform surface temperature condition clearly meant different values of heat flux for various zones. The experiment was run for different values of airflow rates (i.e. different static pressures), plate spacings and plate surface temperatures. A typical experimental run consisted of the following steps:

1. The Power was switched on.
2. The Plate spacing was fixed at a required value.
3. Flow velocity was adjusted by controlling the power input to the four fans mounted at the top of the apparatus to obtain the required flow rate and the static pressure.
4. Temperatures on the plate surface were monitored using temperature controllers and power to the heaters was adjusted until same steady plate surface temperatures were obtained in each zone. These steady state temperatures were recorded using thermocouples.
5. Relevant parameters were computed.

Chapter 4

RESULTS AND DISCUSSION

4.1 Introduction

Previous chapter described the test rig and its instrumentation to study heat transfer for PCB type configuration. A large volume of data was collected for the uniform temperature of the plate simulating the PCB. This chapter is intended to present the analysis of the same data. Some remarkable trends were observed in the heat transfer parameters like heat flux, Nusselt number profile etc.; these are being highlighted at the appropriate places. Empirical relations were also obtained and described here for the purpose.

4.2 Data Range

<u>Parameter</u>	<u>Values for which data were obtained</u>
1.Surface Temperature	50, 60 and 70°C
2.Plate Spacings	15, 20, 30, 40, 50, 60 and 70mm
3.Static Pressure Difference	1.6, 2.4, 5.4, 9.6 and 15 Pa

4.3 Heat Dissipation by Natural Convection

4.3.1 Nusselt Number Versus Rayleigh Number

Figure 4.1 shows variation in Nusselt number with Rayleigh number for pure natural convection situation for different uniform surface temperatures. The plot clearly shows a substantial increase in Nusselt Number as uniform surface temperature was increased. This increase in Nusselt Number was attributed primarily to high heat input required to maintain high surface temperatures.

On the other hand for a given uniform surface temperature there was no substantial variation in the value of Nusselt Number with respect to Rayleigh Number (signifying the effect of buoyancy) except at the lower range of the data. These relatively high values of Nusselt Numbers may be due to high-induced flow at lower plate spacings. Increase in plate spacing slightly decreased the induced flow velocity, which resulted in a decreasing trend of the curve and finally approaching a constant value of the Nusselt Number.

4.3.2 Effect of Plate Spacing

Figure 4.2 shows the variation of plate heat flux with respect to plate spacing at different uniform surface temperatures. The plot clearly shows the increase in heat flux value as surface temperature was increased. This increase in heat flux value was attributed to high heat input required in order to maintain high surface temperature.

As can be seen from the figure, for a given surface temperature, heat flux value does not vary much. It shows that after certain spacing heat flux can not be enhanced just

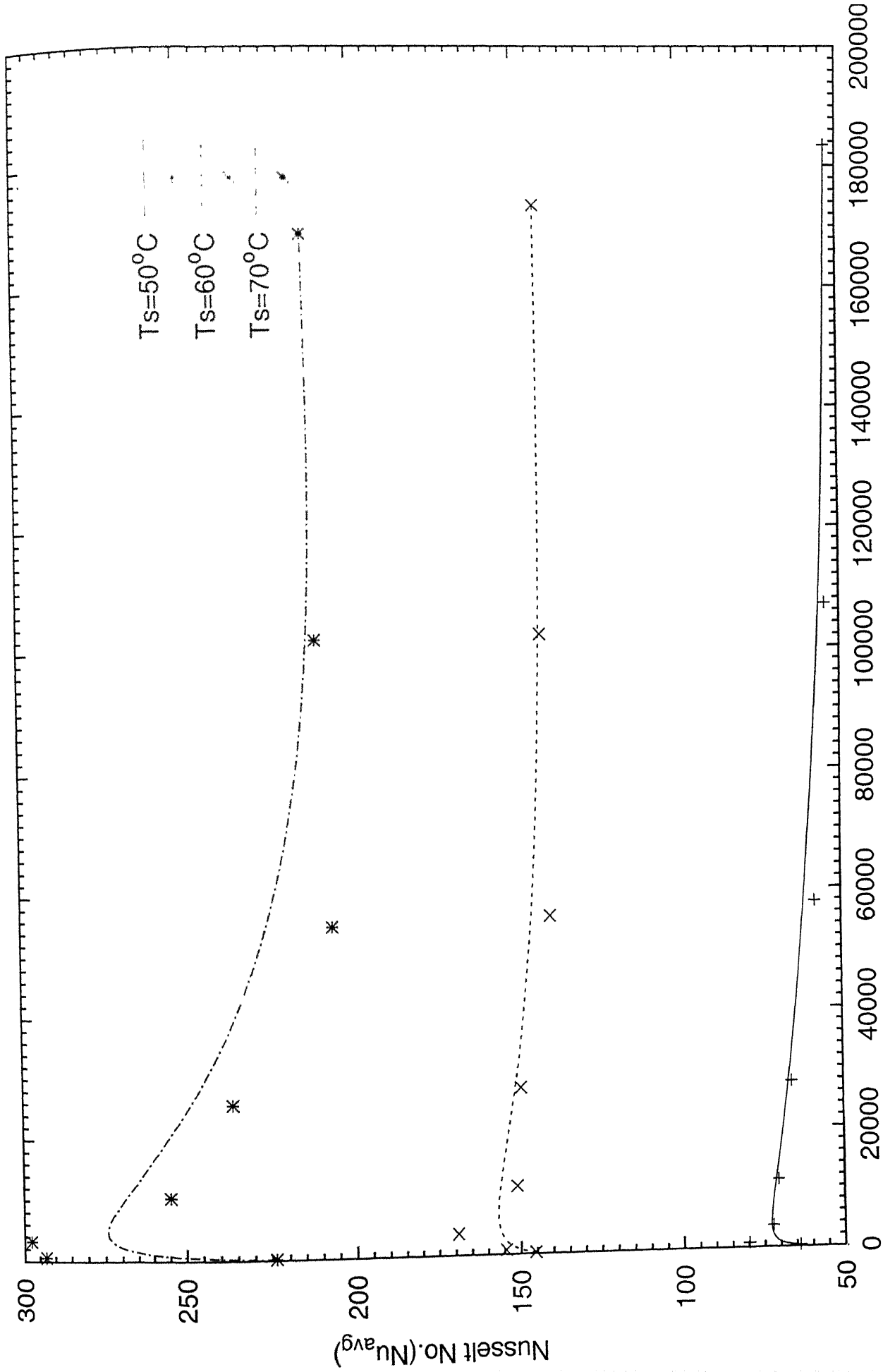


Fig 4.1: Nusselt No. versus Rayleigh No.

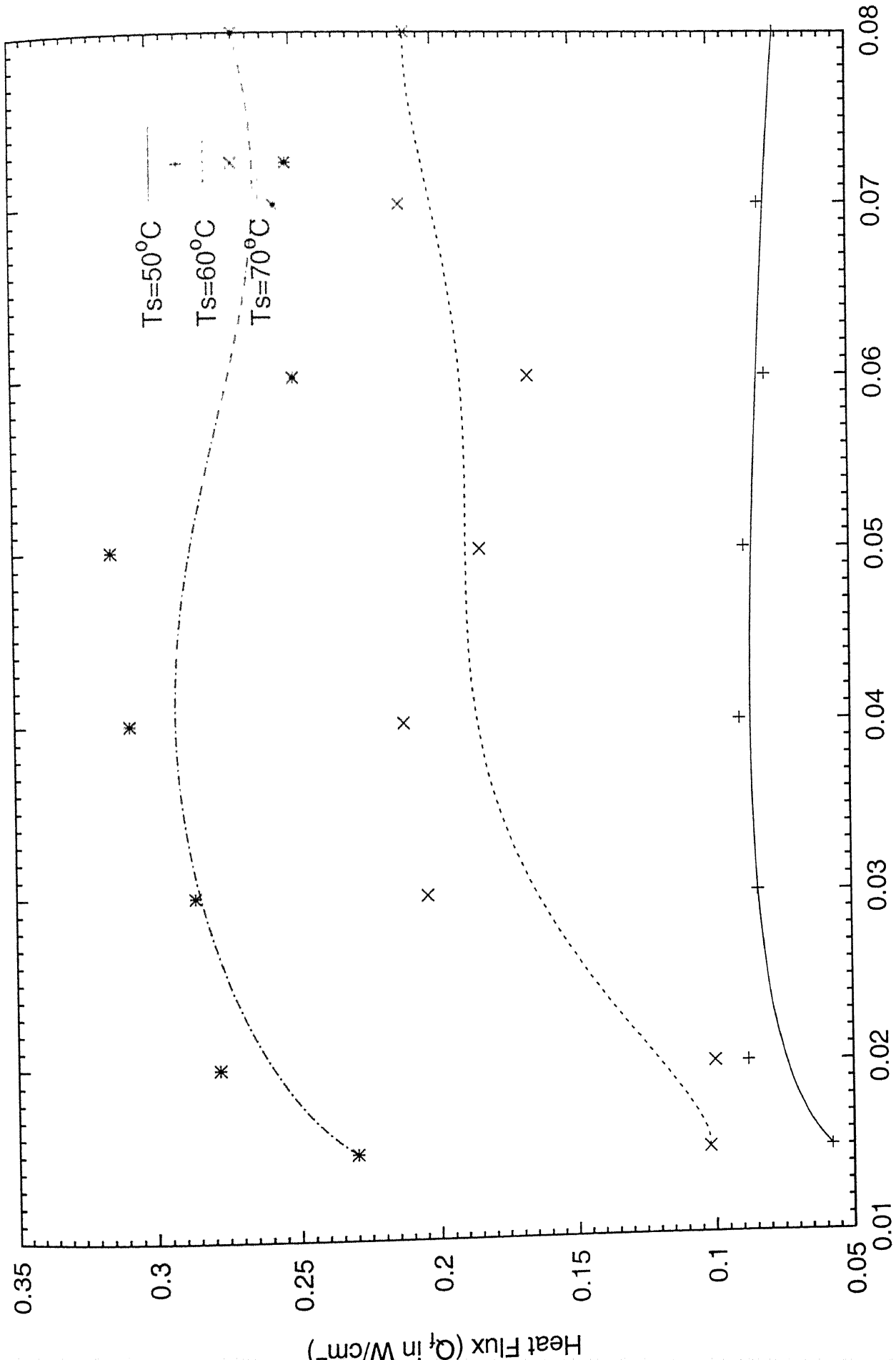


Plate Spacing (X in m)

Fig 4.2: Heat Flux versus Plate Spacing

by increasing the spacing. The figure shows that there is a limitation up to which heat can be dissipated by natural convection. In order to enhance it further one has to resort to some other cooling methods. One of them which can help increase the heat dissipation is Mixed convection i.e. heat transfer by using both natural as well as forced convection by providing sufficient static pressure across the channel to be cooled.

4.4 Heat Dissipation by Mixed Convection

4.4.1 Effect of Plate Spacing on Nusselt Number

Figure 4.3 shows the variation of the Nusselt number with plate spacing for different values of the fan static pressures. These data were taken for plate surface temperature $T_s=50^{\circ}\text{C}$. It can be observed from figure 4.3 that for the static pressure values at the lower side, Nusselt number almost remained around 500. As the Static pressure value was increased above 5.0 Pa, Nusselt number no longer remained constant for small plate spacings (say up to, 30 mm) beyond which it increased and then decreased and approached a constant value as the spacing was increased. It may be noted that for higher static pressures, the initial slopes of curves tended to increase. For UWT of 50°C , maximum achievable value of Nusselt number was around 5400, which corresponded to a static pressure of 15 Pa and plate spacing of about 15 mm.

Figure 4.4 shows the variation of Nusselt number with plate spacing at wall temperature of 60°C . The Nusselt number had a slightly higher value at lower spacing and lower static pressure as can be seen by comparing the curve for 2.4 Pa in this plot with that shown in figure 4.3. The Nusselt number invariably tended to achieve constant values for various

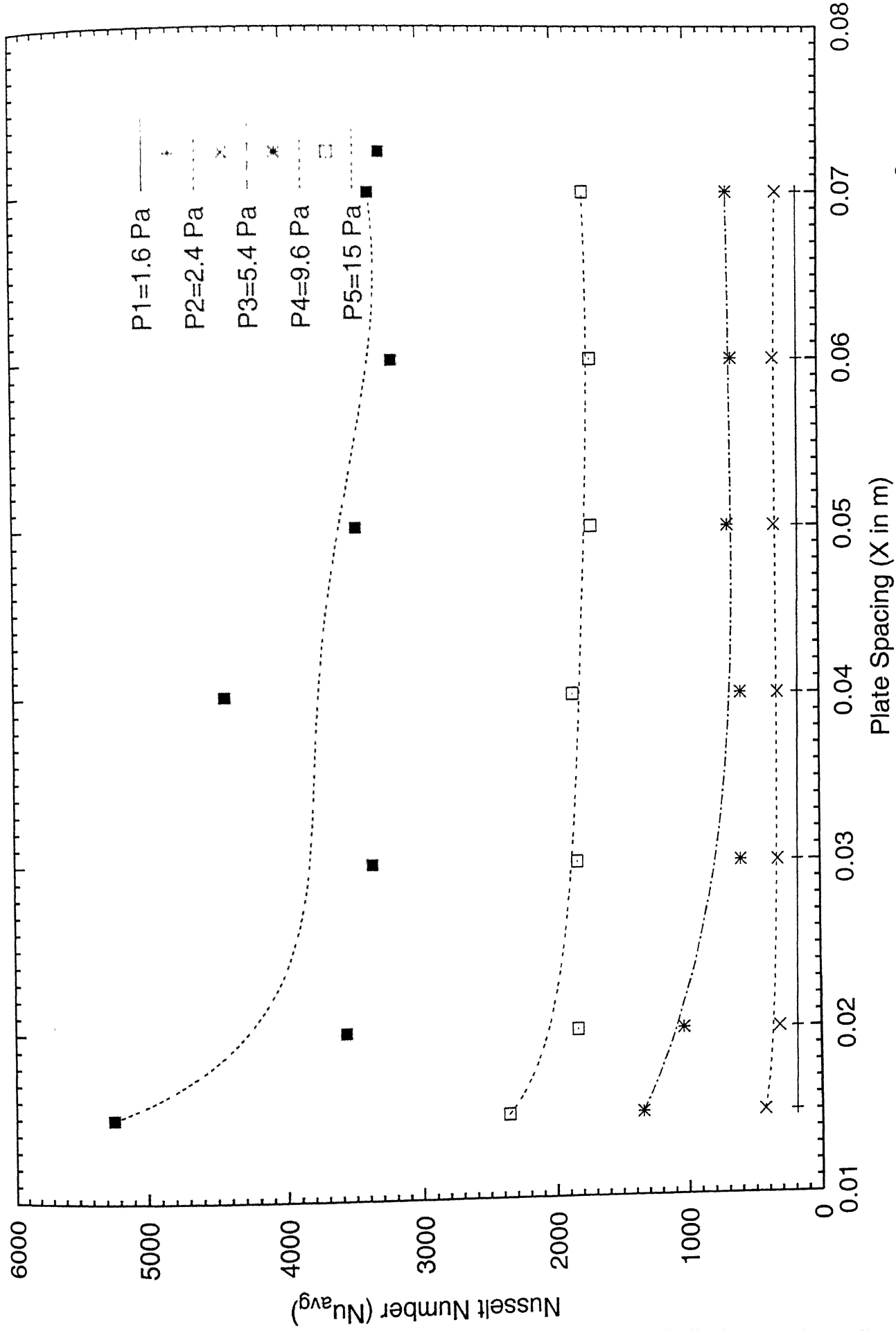


Fig 4.3: Nusselt No. versus Plate Spacing for different Static Pressures ($T_s = 50^\circ\text{C}$)

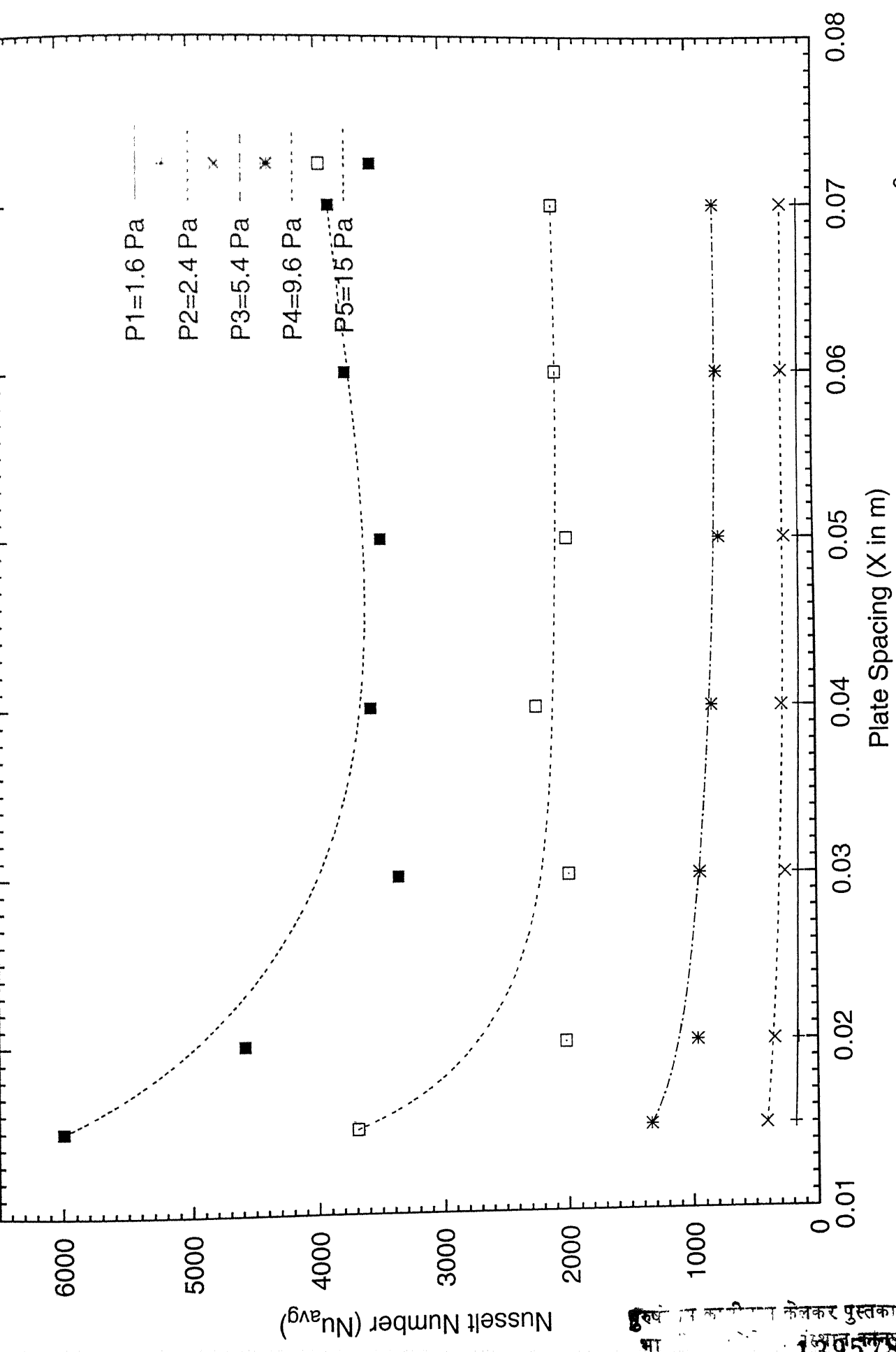


Fig 4.4: Nusselt No. versus Plate Spacing for different Static Pressures ($T_s = 60^\circ\text{C}$)

static pressures. The maximum value of Nusselt number was about 6000 for static pressure of 15.0 Pa and plate spacing of 20 mm, however maximum limiting value of Nusselt number was around 3800.

Figure 4.5 also shows variation of Nusselt number with plate spacing for different static pressures at the UWT of 70°C. It can be clearly seen that Nusselt number invariably increased with the increase in static pressure. As compared to the characteristics shown in figures 4.4 and 4.3, some increase in Nusselt number could be seen even at lower pressure values like 1.6 Pa. At smaller spacing, the Nusselt number value was substantially higher, but it approached a lower limiting value as the plate spacing was increased. The Maximum values of Nusselt number were noted at plate spacing around 15 mm for different static pressures. For UWT of 70°C, overall maximum value of Nusselt number was around 4400 and the steady state maximum value was about 4000.

4.4.2 Effect of Plate Spacing on Heat Flux

Figure 4.6 shows variation in heat flux (W/cm^2) with plate spacing and varying static pressures for a plate temperature of 50°C. The heat flux undoubtedly increased with an increase in static pressure, but the effect of plate spacing variation over heat flux was difficult to analyze in a straightforward manner. One thing that was clearly observed was that for some initial values of spacing (between 15mm and 40mm), the flux approached some peak value before showing oscillations. In the parametric range under consideration the maximum value of heat flux occurred at static pressure of 15.0 Pa and spacing of around 30 mm.

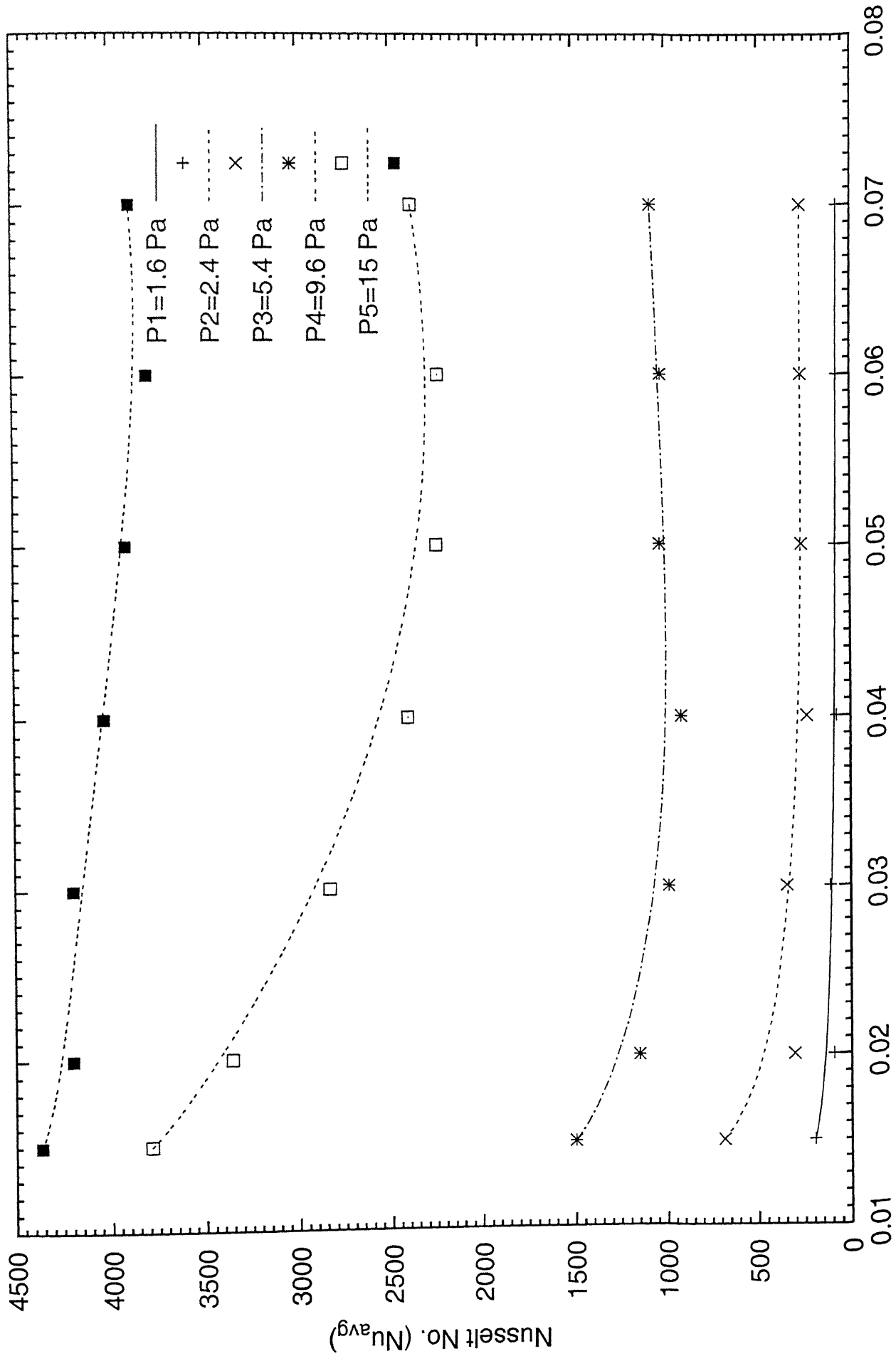


Plate Spacing (X in m)

Fig 4.5: Nusselt No. versus Plate Spacing for different Static Pressures ($T_s=70^\circ\text{C}$)

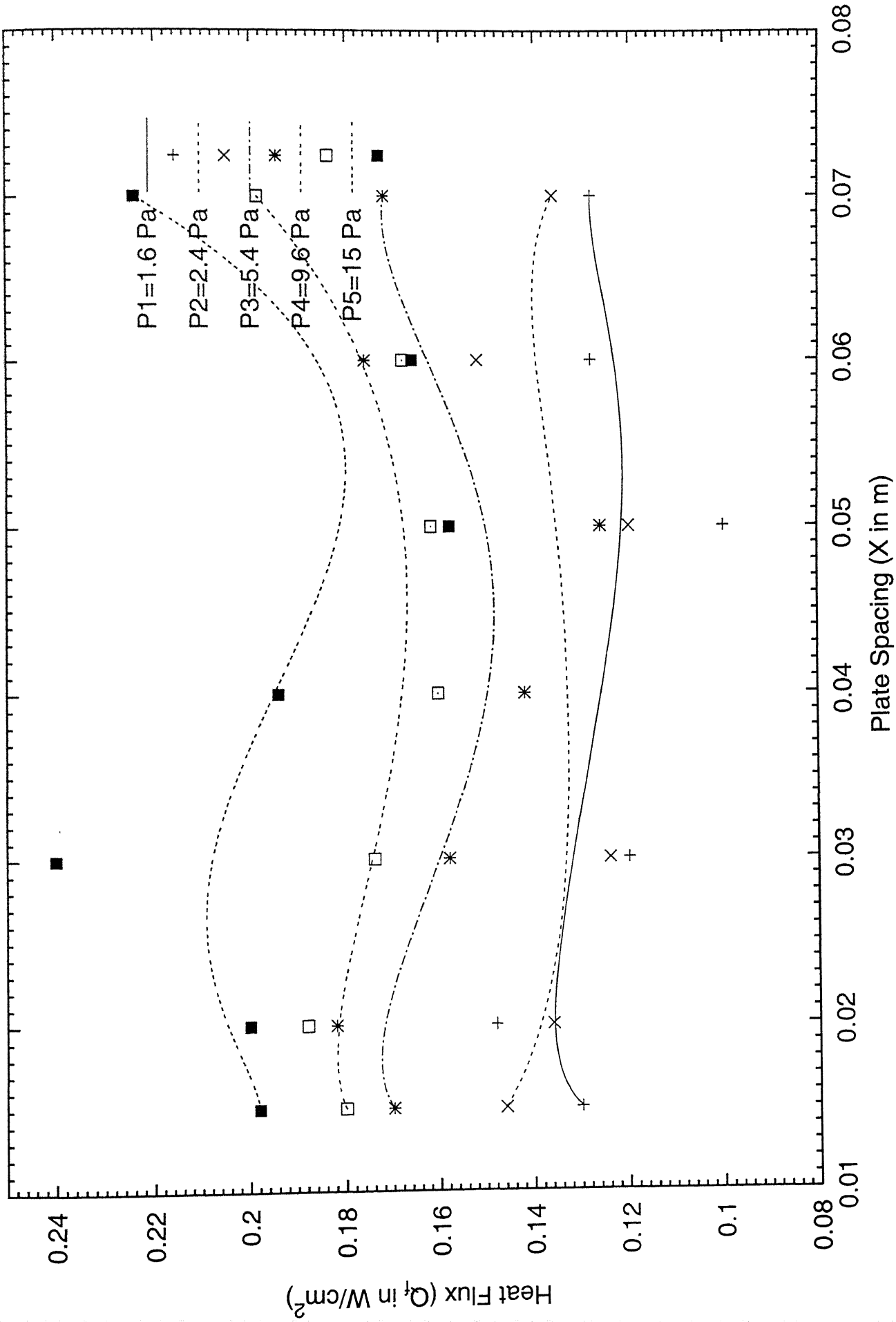


Fig 4.6: Heat Flux versus Plate Spacing for different Static Pressures ($T_s=50^\circ\text{C}$)

Figure 4.7 shows the heat flux variation with the plate spacing for different values of static pressure. The UWT was maintained at 60°C. Heat flux invariably increased with increase in static pressure. Heat flux values were highest at the minimum value of plate spacing (near 15 mm). The heat flux first decreased sharply with increase in plate spacing and then attained a constant value. The apparent increase in heat flux value for the larger plate spacing was mainly due to some instrumentation and measurement inaccuracies rather than due to some physical reason. The maximum value of heat flux was about 0.35 W/cm², which could be achieved for static pressures between 10 and 15 Pa depending on the plate spacing. For the larger plate spacing the steady state value was near about 0.3 W/cm².

Figure 4.8 shows the variation of heat flux with plate spacing for different values of static pressure. The UWT was maintained at 70°C. The pattern followed by the heat flux was more or less similar to figure 4.7. The value of heat flux invariably increased with the increase in static pressure. At the low static pressures, the variation in heat flux for different plate spacing was relatively low and gradually increased with increase in it. The maximum value of heat flux achieved at UWT of 70°C was about 0.45 W/cm² at a plate spacing of about 15 mm and at a static pressure of 15.0 Pa. The maximum steady state value for the heat flux was around 0.43 W/cm² for the same static pressure.

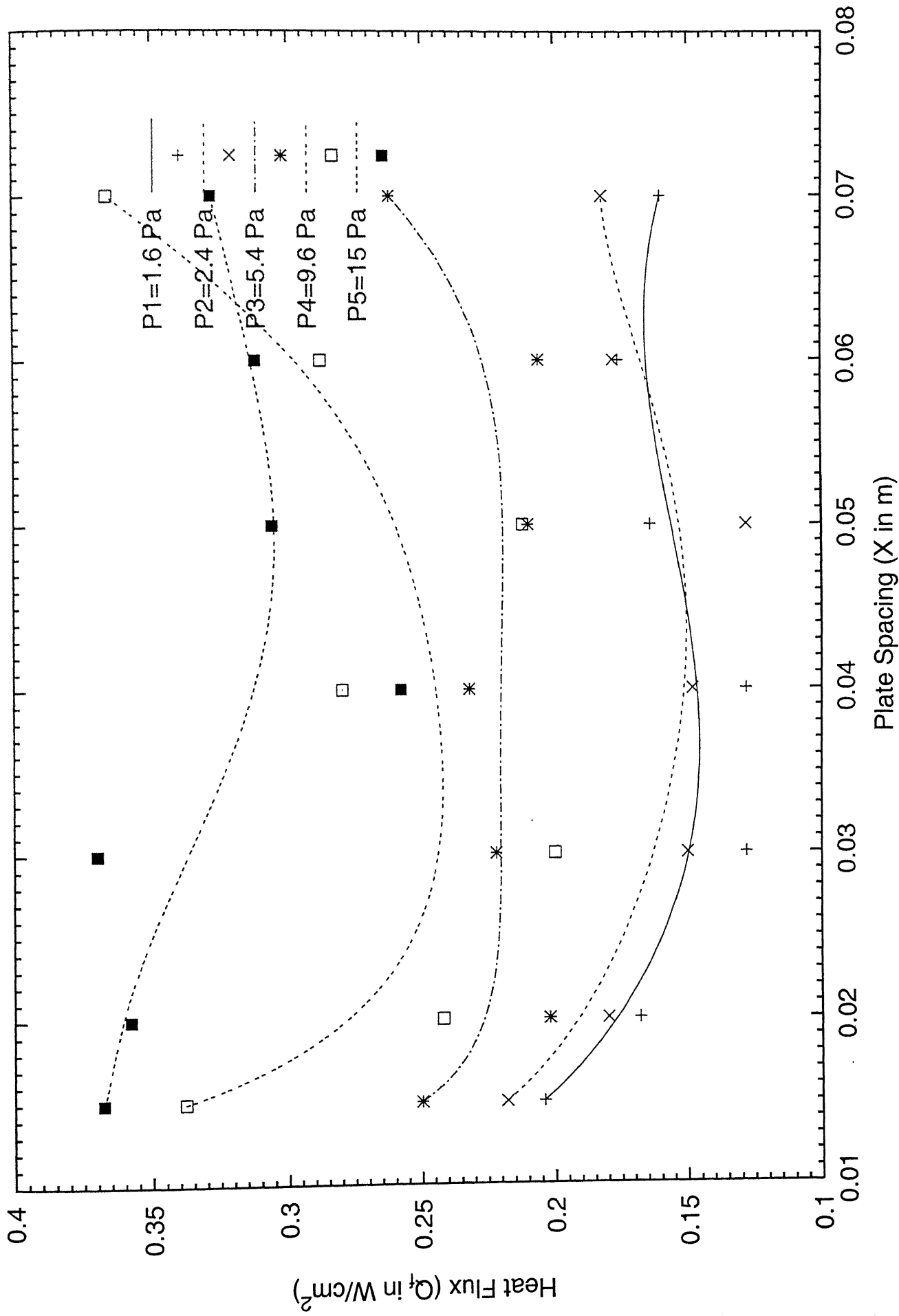


Fig 4.7: Heat Flux versus Plate Spacing for different Static Pressures ($T_s=60^\circ C$)

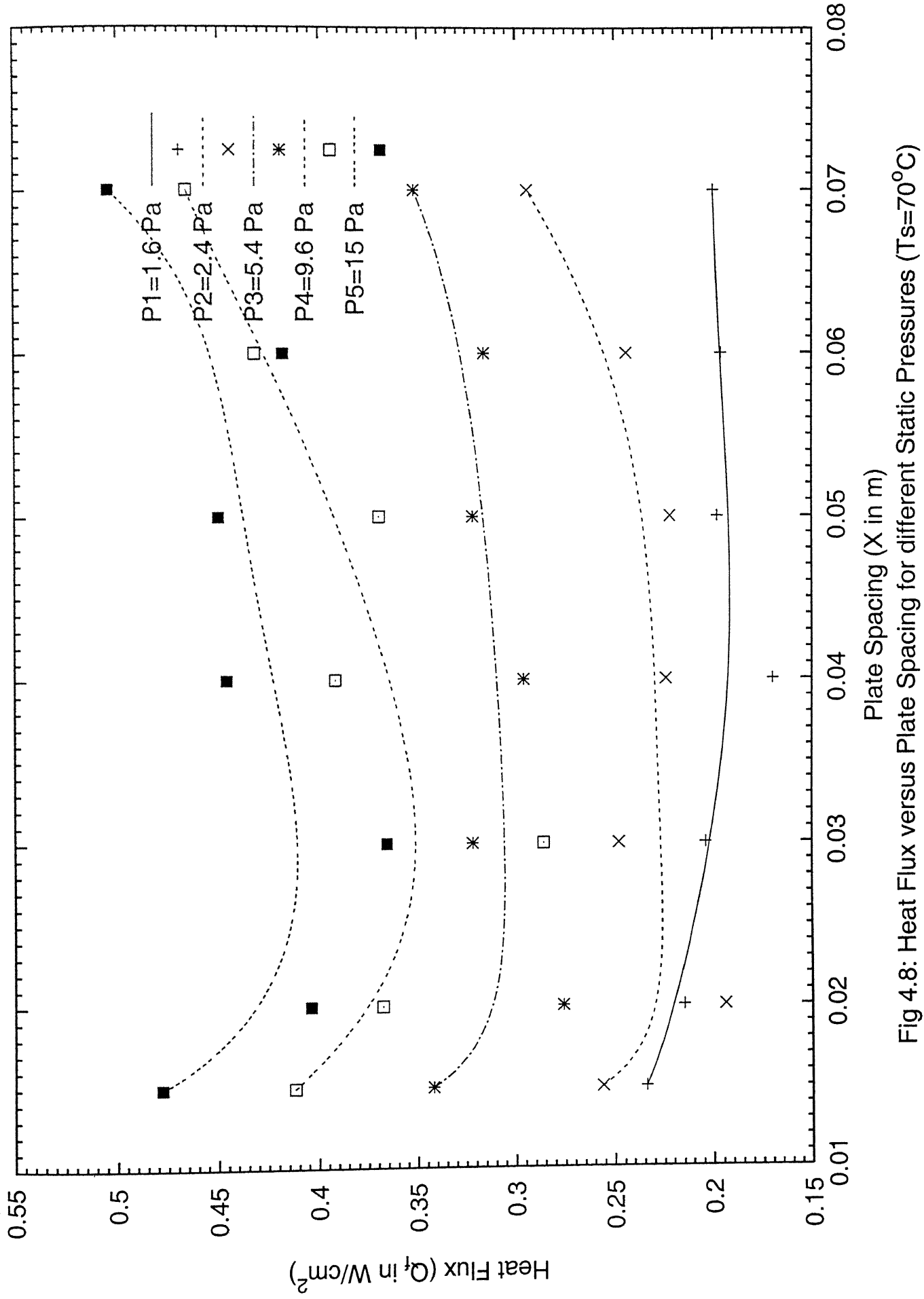


Fig 4.8: Heat Flux versus Plate Spacing for different Static Pressures ($T_s=70^\circ C$)

4.5 Effect of Static Pressure on Optimum Spacing

By optimum spacing we precisely mean that the value of plate spacing for which either the value of heat flux was maximum or the corresponding change in heat flux for further increase or decrease in the plate spacing was not substantial. In fact, the optimum spacing is a very important parameter in deciding the thermal design of electronic equipment consisting of a number of PCB's. By thermal design we basically mean arrangement of predesigned PCBs in that particular equipment.

Figure 4.9 shows the variation of optimum spacing with static pressure for different plate surface temperatures. It can be observed from the figure that for a static pressure below 4.0 Pa, the optimum spacing more or less increased with decrease in pressure. The maximum value of the optimum spacing occurred for the natural convection i.e. when the static pressure was zero. Maximum optimum spacing value was 45 mm for the plate surface temperature of 70°C. Below 2.0 Pa, static pressure, the optimum spacing increased with increase in plate surface temperature. Above this value of static pressure, there was sudden change in trend and the optimum spacing was found to decrease with increase in plate surface temperature. This trend of the data seemed to be unrealistic and needed further experimentation. If the measurement errors are accounted for, it may be easy to conclude that the optimum spacing tended to approach some limiting value for each plate temperature as the static pressure increased beyond 4.0 Pa.

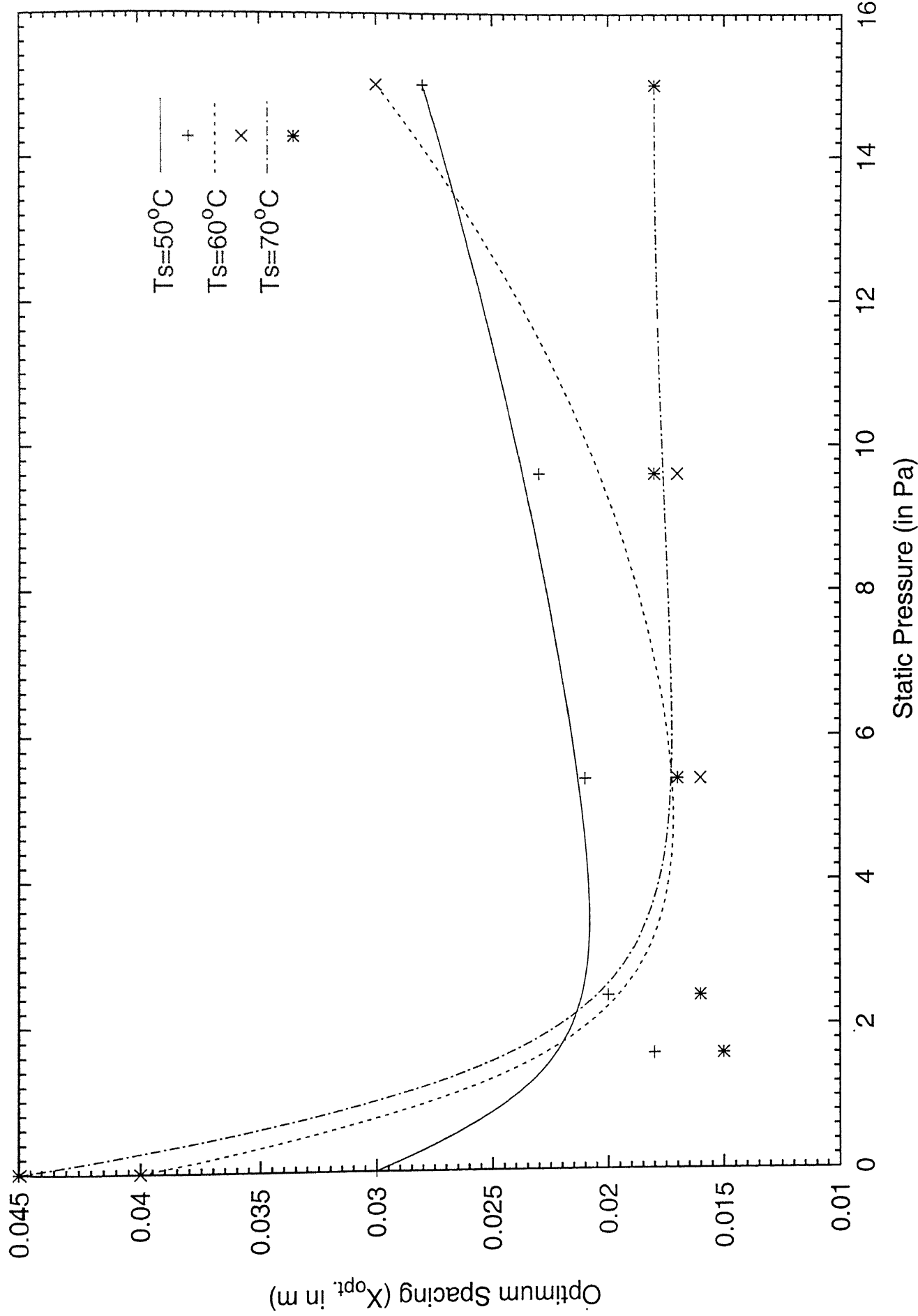


Fig 4.9: Optimum Spacings versus Static Pressures for different Plate Surface Temperatures

4.6 Effect of Static Pressure on Optimum Heat Flux

Optimum heat flux refers to heat flux value corresponding to the optimum spacing which was the maximum achievable heat flux if the plate spacing was varied along with the static pressure. Figure 4.10 shows the variation in optimum heat flux with change in static pressure for different plate surface temperatures. It can be observed that the value of optimum heat flux increased with increase in plate surface temperature as well as with increase in static pressure. For UWT of 50°C, optimum heat flux was found to first increase suddenly and then vary linearly with the increase in static pressure. At this temperature and static pressure of 15.0 Pa, the maximum value of heat flux was around 0.17 W/cm².

For the plate surface temperatures of 60°C and 70°C the optimum heat flux increased almost linearly (starting from 0.19 and 0.29 W/cm² respectively) with the increase in static pressure. Maximum value of heat flux for these two temperatures at 15.0 Pa was around 0.30 and 0.48 W/cm² respectively.

4.7 Correlation

Suggested correlations for optimum Spacing and optimum heat flux are as follows:

$$X_{opt} = \left(0.005 + \frac{T - 50}{1000} \right) + \left[0.001 + (T - 50) \times 10^{-5} \right] P + (0.01) \log \left[\frac{1}{P + 0.12} + 5^{6 - 0.1T} \right]$$

$$Q_{opt} = T \times 10^{-2} + P \times 8.5 \times 10^{-3} - 0.40$$

Where:

$$15 \leq X \leq 70, 50 \leq T \leq 70, 0 \leq P \leq 15$$

X_{opt} is in m., T is in °C, P is in Pa and Q_{opt} is in W/cm²

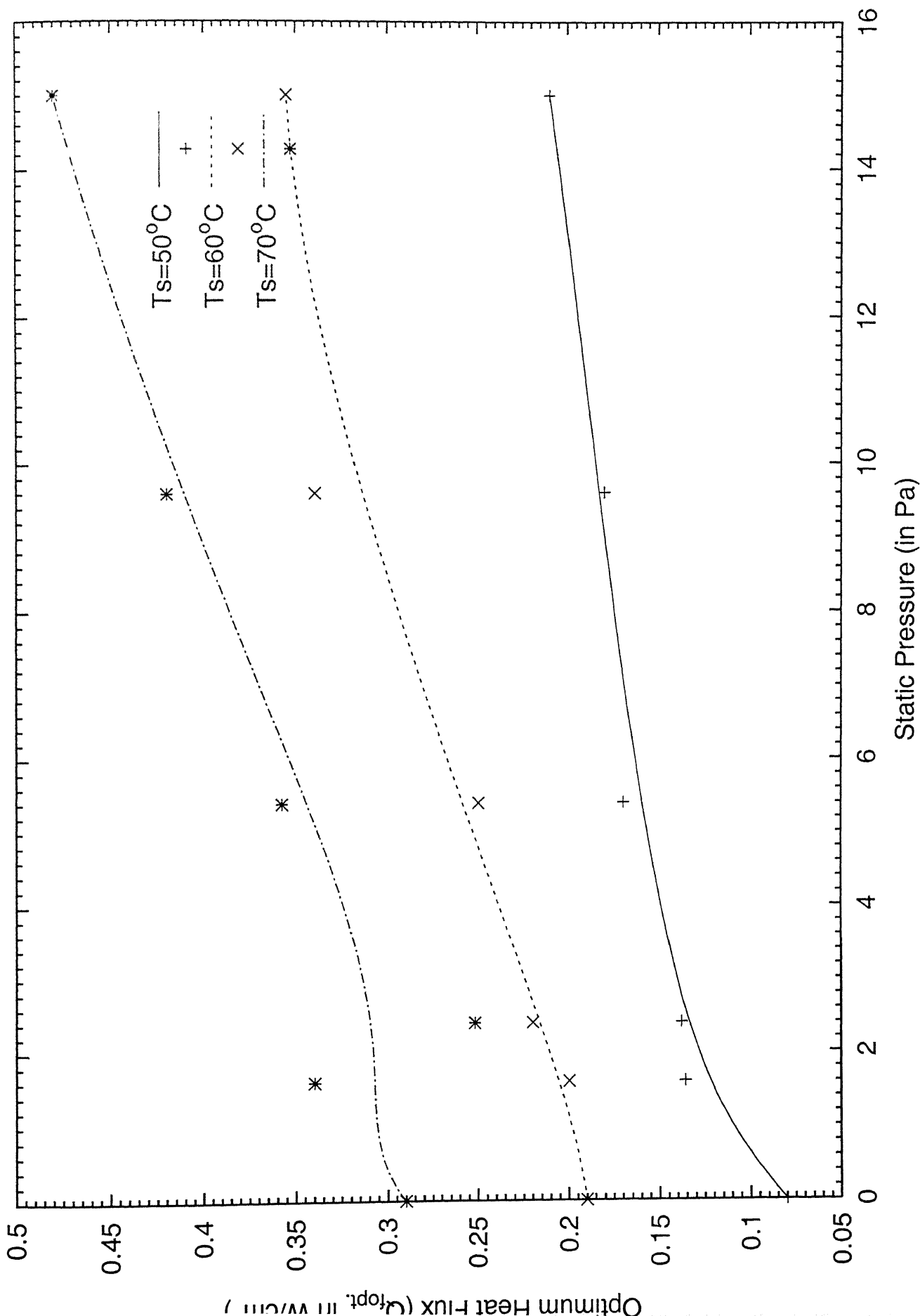


Fig 4.10: Optimum Heat Flux versus Static Pressures for different Plate Surface Temperatures

4.8 Error Analysis

Due to certain inaccuracy in the data acquired, errors in the final results are inevitable. Different instruments have different inaccuracies, which get compounded in the final results. The knowledge of inaccuracy of different instruments used in the current experimental study and the associated errors introduced in the subsequently calculated quantities are very important before one can really appreciate the experimental results. Some of the important information related to experimental inaccuracies is listed below:

Table 4.1

S.No.	Instruments	Accuracy	Associated Reading	Error
1.	Microvolt meter	± 0.5 %fsd	Temperature ($^{\circ}\text{C}$)	± 0.5 %
2.	Vane anemometer	± 0.25 %fsd	Flow velocity (v)	± 0.25 %
3.	Gap Scale	1.0 %	Plate spacing (m)	1.0 %
4.	Temperature Controllers	± 2.0 %	Temperature ($^{\circ}\text{C}$)	± 2.0 %

Table 4.2

S.No.	Calculated Parameter	Percent Error
1.	Nusselt No.	± 1.5 %
2.	Rayleigh No.	± 5.0 %
3.	Heat Flux	± 0.5 %

the plate spacing indicating some limiting value at higher static pressures. Additional experimentation can throw more light on this aspect. Optimum Heat flux was found to have a higher value for the larger UWT and more or less linear increment with increase in static pressure values.

4. Two empirical relations for optimum plate spacing and optimum heat flux were also presented.

4.10 Scope for Future Work

The Uniform Wall Temperature condition can be achieved more effectively by dividing the heated plate in a larger number of heated strips and thus incorporating a large number of heaters. This requires use of a good Data Acquisition and Feedback Control System. The uniform plate temperature value requires having a broad range supposedly between 60°C to 150°C . The range of plate spacing and the static pressure also need to be increased beyond the range considered. A very good quality work can be pursued if different types of temperature profiles are considered over the plate surface.

REFERENCES

- 1- Min-Joon Kim, Young-Bum Lee, Young-Kyun Kim, Byoung-Hae Choi and Ho-Yun Nam. 2001, 'Mixed convection in an unequally heated loop: Steady solutions', **Int. J. of Heat and Mass Transfer**, Vol. 44, pp 389-397.
- 2- Tewari, S.S. and Jaluria, Y., 1991, 'Mixed convection heat transfer from thermal sources mounted on horizontal and vertical surfaces', **Journal of Heat Transfer Trans. ASME**, Vol. 112, pp 975-987.
- 3- Chen, Y.-C., and Chung, J.N., 1998, 'Stability of mixed convection in a differentially heated vertical channel', **Journal of Heat Transfer Trans. ASME**, Vol. 120, pp 127-132.
- 4- Tso, C.P., Xu, G.P., and Tou, K.W., 1999, 'An experimental study on forced convection heat transfer from flush mounted discrete heat sources', **Journal of Heat Transfer Trans. ASME**, Vol. 121, pp 326-332.
- 5- Tseng, W.S., Lin, W.L., Yin, C.P., and Lin, T.F., 2000, 'Stabilization of buoyancy-driven unstable vortex flow in mixed convection of air in a rectangular duct by tapering its top plate', **Journal of Heat Transfer Trans. ASME**, Vol. 122, pp 58-65.
- 6- Zhang, X., and Dutta, S., 1998, 'Heat transfer analysis of buoyancy-assisted mixed convection with assymmetric heating conditions', **Int. J. of Heat and Mass Transfer**, Vol. 41, pp 3255-3264.
- 7- Ligrani, P.M., and Choi, S., 1996, 'Mixed convection in straight and curved channels with buoyancy orthogonal to the forced flow', **Int. J. of Heat and Mass Transfer**, Vol. 39, pp 2473-2484.

- 8- Gau, C., Huang, T.M., and Aung, W., 1996, 'Flow and mixed convection heat transfer in a divergent heated vertical channel', **Journal of Heat Transfer**, Vol. 118, pp 606-615.
- 9- Maughan, J.R., and Incropera, F.P., 1990, 'Regions of heat transfer enhancement for mixed convection in a parallel plate channel', **Int. J. of Heat and Mass Transfer**, Vol. 33, pp 555-570.
- 10- Maughan, J.R., and Incropera, F.P., 1987, 'Experiments on mixed convection heat transfer for air flow in a horizontal and inclined channel', **Int. J. of Heat and Mass Transfer**, Vol. 30, pp 1307-1318.
- 11- Ramachandran, N., Armaly, B.F., and Chen, T.S., 1995, 'Measurements and production of laminar mixed convection flow adjacent to a vertical surface', **Journal of Heat Transfer Trans. ASME**, Vol. 107, pp 636-641.
- 12- Yadav, V., Kumar, M. and Kant, K., 2002, 'An Experimental Search for Optimum Spacing in Mixed Convection cooling of Electronic PCB's ', **Proc. 16th ISHMT and 5th ISHMT-ASME Heat and Mass Transfer conference held at Kolkata**, pp 493-499.
- 13- Rao, C.G., C. Balaji and S.P. Venkateshan, 2001, 'Conjugate Mixed convection with surface Radiation from a vertical plate with a discrete heat source', **Journal of Heat Transfer Trans. ASME**, Vol. 123, pp 698-702.
- 14- Papnicolaou, E. and Jaluria, Y., 1994, 'Mixed convection from simulated electronic component at varying relative positions in a cavity', **Journal of Heat Transfer Trans. ASME**, Vol. 116, pp 960-970.

- 15- Davalath, J. and Bayazetogue, Y., 1987, 'Forced convection air cooling across rectangular blocks', **Journal of Heat Transfer Trans. ASME**, Vol.109, pp 321-328.
- 16- Barletta, A., 2000, 'Combined free and forced flow for a power-law fluid in a vertical annular duct', **Int. J. of Heat and Mass Transfer**, Vol. 43, pp 3673-3686.
- 17- Monkalled, F., Doughan, A., and Acharya, S., 2000, 'Parametric study of mixed convection in a channel with concave and convex surfaces', **Int. J. of Heat and Mass Transfer**, Vol. 43, pp 1947-1963.
- 18- Yadav, V., and Kant, K., 2000, 'Optimum static pressure in mixed convection cooling in a stack of heated plates', **Proc. 15th ISHMT and 4th ISHMT-ASME Heat and Mass Transfer Conference**, pp 623-630.
- 19- Cheng, C.H., and Lin, C.Y., 2000, 'Predictions of developing flow with buoyancy assisted flow separation in a vertical rectangular duct : parabolic model versus elliptic model', **Numerical heat transfer**, Vol. 37, pp 567-586.

A 139578

